

## Article

# New Nucleic Base-Tethered Trithiolato-Bridged Dinuclear Ruthenium(II)-Arene Compounds: Synthesis and Antiparasitic Activity

Oksana Desiatkina <sup>1</sup>, Martin Mösching <sup>1</sup>, Nicoleta Anghel <sup>2</sup>, Ghalia Boubaker <sup>2</sup>, Yosra Amdouni <sup>2,3</sup> , Andrew Hemphill <sup>2,\*</sup> , Julien Furrer <sup>1,\*</sup>  and Emilia Păunescu <sup>1,\*</sup>

<sup>1</sup> Department of Chemistry, Biochemistry and Pharmaceutical Sciences, University of Bern, Freiestrasse 3, 3012 Bern, Switzerland

<sup>2</sup> Institute of Parasitology, Vetsuisse Faculty, University of Bern, Länggass-Strasse 122, 3012 Bern, Switzerland

<sup>3</sup> Laboratoire de Parasitologie, Institution de la Recherche et de l'Enseignement Supérieur Agricoles, Université de la Manouba, École Nationale de Médecine Vétérinaire de Sidi Thabet, Sidi Thabet 2020, Tunisia

\* Correspondence: andrew.hemphill@vetsuisse.unibe.ch (A.H.); julien.furrer@unibe.ch (J.F.); paunescu\_emilia@yahoo.com (E.P.); Tel.: +41-31-6842384 (A.H.); +41-31-6844383 (J.F.); Fax: +41-31-6312477 (A.H.)

**Abstract:** Aiming toward compounds with improved anti-*Toxoplasma* activity by exploiting the parasite auxotrophies, a library of nucleobase-tethered trithiolato-bridged dinuclear ruthenium(II)-arene conjugates was synthesized and evaluated. Structural features such as the type of nucleobase and linking unit were progressively modified. For comparison, diruthenium hybrids with other type of molecules were also synthesized and assessed. A total of 37 compounds (diruthenium conjugates and intermediates) were evaluated in a primary screening for in vitro activity against transgenic *Toxoplasma gondii* tachyzoites constitutively expressing  $\beta$ -galactosidase (*T. gondii*  $\beta$ -gal) at 0.1 and 1  $\mu$ M. In parallel, the cytotoxicity in non-infected host cells (human foreskin fibroblasts, HFF) was determined by alamarBlue assay. Twenty compounds strongly impairing parasite proliferation with little effect on HFF viability were subjected to *T. gondii*  $\beta$ -gal half maximal inhibitory concentration determination (IC<sub>50</sub>) and their toxicity for HFF was assessed at 2.5  $\mu$ M. Two promising compounds were identified: **14**, ester conjugate with 9-(2-oxyethyl)adenine, and **36**, a click conjugate bearing a 2-(4-(hydroxymethyl)-1H-1,2,3-triazol-1-yl)methyl substituent, with IC<sub>50</sub> values of 0.059 and 0.111  $\mu$ M respectively, significantly lower compared to pyrimethamine standard (IC<sub>50</sub> = 0.326  $\mu$ M). Both **14** and **36** exhibited low toxicity against HFF when applied at 2.5  $\mu$ M and are candidates for potential treatment options in a suitable in vivo model.

**Keywords:** ruthenium(II)-arene complexes; CuAAC reactions; antiparasitic compounds; *Toxoplasma gondii*; human foreskin fibroblasts; toxicity; auxotrophy; nucleic bases



**Citation:** Desiatkina, O.; Mösching, M.; Anghel, N.; Boubaker, G.; Amdouni, Y.; Hemphill, A.; Furrer, J.; Păunescu, E. New Nucleic Base-Tethered Trithiolato-Bridged Dinuclear Ruthenium(II)-Arene Compounds: Synthesis and Antiparasitic Activity. *Molecules* **2022**, *27*, 8173. <https://doi.org/10.3390/molecules27238173>

Academic Editor: Mihaela Badea

Received: 8 November 2022

Accepted: 22 November 2022

Published: 24 November 2022

**Publisher's Note:** MDPI stays neutral with regard to jurisdictional claims in published maps and institutional affiliations.



**Copyright:** © 2022 by the authors. Licensee MDPI, Basel, Switzerland. This article is an open access article distributed under the terms and conditions of the Creative Commons Attribution (CC BY) license (<https://creativecommons.org/licenses/by/4.0/>).

## 1. Introduction

*Toxoplasma gondii*, the most prevalent infectious protozoan in man, is an opportunistic pathogen with a high zoonotic potential. Approximately 30% of humans worldwide, as well as most warm-blooded animal species, are infected with this parasite [1,2]. Acute toxoplasmosis can be life-threatening in immunocompromised hosts, and upon primary infection during pregnancy, the parasite can cross the placenta and inflict fetal damage and/or abortion [3], rendering *T. gondii* an important public health problem [2,4]. Current management of toxoplasmosis relies on conventional therapy, which has important shortcomings related to reduced tolerance and overall potency, poor efficacy to the latent stage of the parasite, as well as drug resistance [5,6].

As an obligate intracellular pathogen that can invade and replicate in any nucleated mammalian cell, *T. gondii* is in stringent dependence on specific host cell resources [7].

The parasite lacks many genes encoding the entire metabolic pathways, but has evolved efficient strategies to acquire crucial metabolites from the host cells [8]. For survival, *T. gondii* is auxotrophic for numerous nutrients and has acquired salvage mechanisms to import the vital compounds that it cannot synthesize, such as, for example, various metabolites including polyamines, cholesterol, purine derivatives, and essential amino acids [8]. *T. gondii* is a strictly purine (adenine, guanine, xanthine, and hypoxanthine) auxotroph, and is thus incapable of de novo biosynthesis of purine nucleic bases and relies on their scavenging from the host cell to meet its nutritional needs [8–12]. In contrast, *T. gondii* scavenges and synthesizes pyrimidine nucleobases and nucleosides [8,13–16].

The drugs that are currently used for the treatment of toxoplasmosis include antifolates, such as combined pyrimethamine–sulfadiazine or trimethoprim–sulfamethoxazole. Pyrimethamine can be combined with antibiotics that inhibit protein synthesis such as clindamycin and azithromycin, and atovaquone, a mitochondrial cytochrome *bc1* inhibitor that interferes in oxidative phosphorylation, is also in clinical use. However, these treatments are unspecific, adverse effects have been frequently documented, and clinical failures have been reported [17]. A considerable effort is being made to identify better solutions [17–20] and new structures are emerging [21–27]. For example, experimental compounds such as bumped kinase inhibitors, which impair the activity of *T. gondii* calcium dependent protein kinase 1 (essential for host cell invasion and egress), endochin-like quinolones (ELQs) that are specific and potent *T. gondii* cytochrome *bc1* inhibitors, and a leucinoistatin-derived antimicrobial peptide that interferes in multipole metabolic pathways, have been demonstrated to exert anti-parasitic effects in vitro and in vivo [28–30]. In addition, some combinations of pyrimethamine, clindamycin, guanabenz, and ELQs exhibited synergistic effects and were found to be more potent than monotherapies [31].

Chemotherapeutic strategies addressing the parasitic cell cycle and the specific metabolic defects of *T. gondii* based on its auxotrophic nature were explored earlier [32–34]. Targeting the *T. gondii* purine salvage pathways represents a potential pharmacological approach [8,35,36], which was experimentally investigated [37–42] but not widely applied due to the apprehension that compounds affecting parasite metabolism can also be toxic to the host [34]. The potential of purine analogues as antiparasitic agents was previously demonstrated [35,43] and several derivatives have shown efficacy against *T. gondii* [44,45].

The research of metal-based compounds for biological applications has received a lot of attention [46–48], and if initially most of the bioactive metalorganic compounds were conceived as alternatives to anticancer platinum-based drugs [49–51], other pharmacological properties, among which, antiparasitic activity [52–57], further encouraged studies in this area. If ruthenium complexes emerged as one of the most promising classes of metal-based anticancer compounds [58,59], they have also shown particularly interesting efficacy against various parasites [60–65].

Combining two or more active molecules into a hybrid structure is a popular strategy in the design of new therapeutic agents and prior approaches aiming to improve the targeting and anticancer activity of platinum [66,67] and ruthenium [67] complexes by modifying them with metabolites revealed significant benefits [68]. Conjugating metal complexes to nucleobases, nucleosides, and nucleotides afforded compounds with a wide range of applications, such as, for example, potential anticancer agents [69,70]. An important effort was invested in the development of various metallocene–nucleobase hybrids [70–73] and research was further extended to other organometallic derivatives [74–77], some relevant examples being presented in Figure 1.

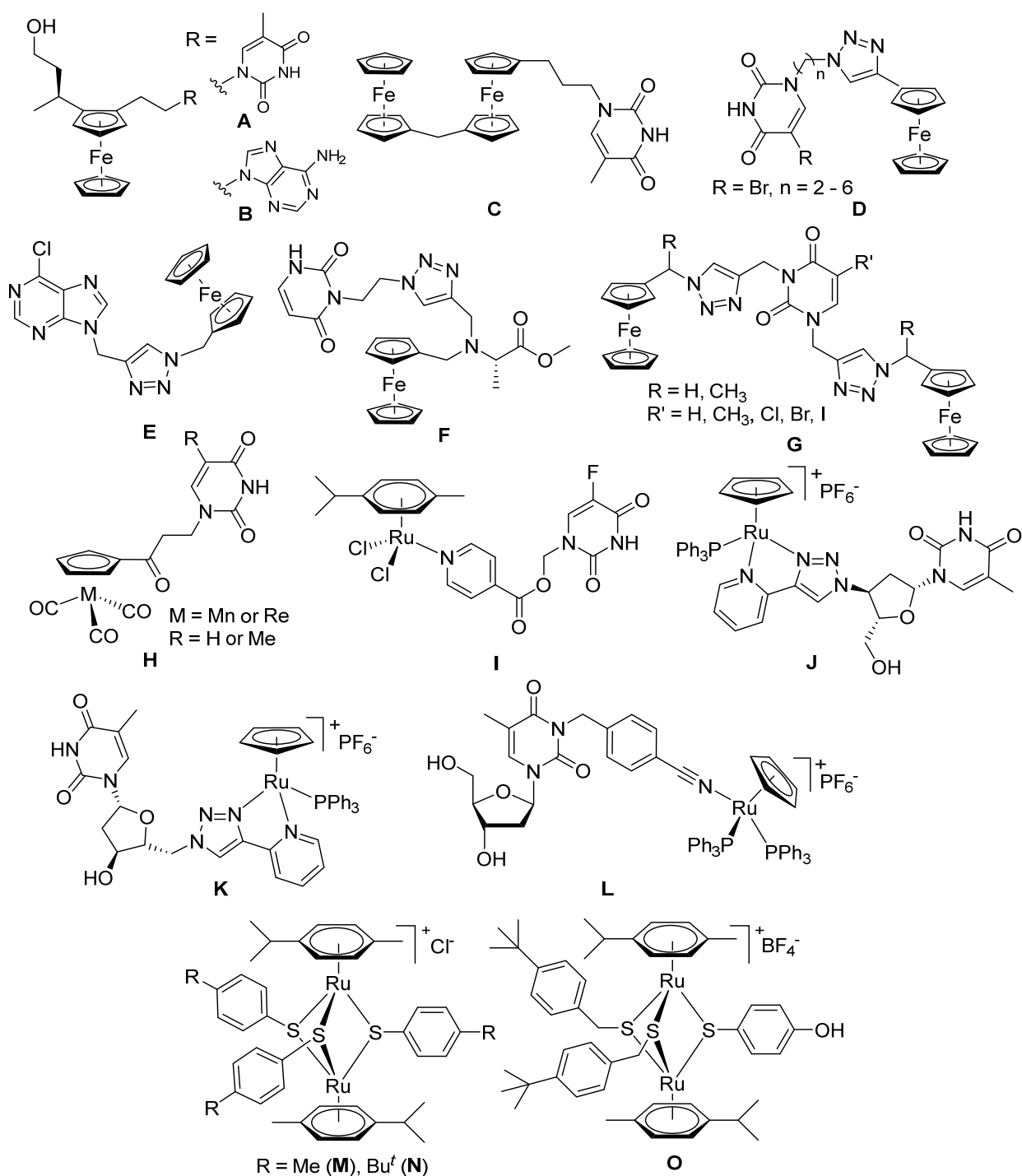


**Figure 1.** Structure of various conjugates organometallic complex nucleobase/nucleoside (A–L), and of symmetric (M,N) and mixed (O) trithiolato-bridged ruthenium(II)-arene complexes.

For example, thymine and adenine ferrocene derivatives **A** and **B** [78,79] and di-ferrocene–uracil compound **C** [80] showed promising anticancer activity and good selectivity. Copper-catalyzed azide-alkyne [3+2] cycloaddition (CuAAC) was used to prepare antitubercular agent **D** [81], anticancer compound **E** [82], and antifungal derivative **F** [72]. CuAAC click reactions also afforded cytostatic bis-ferrocene conjugates **G** bridged by 1,2,3-triazole linkers to 5-substituted uracil [83]. Cymantrene and cyrhetrene uracil and thymine conjugates **H** showed promising activity against *Trypanosoma brucei* and good selectivity [84], and 5-fluorouracil ruthenium(II)-arene compound **I** exhibited moderate

anticancer activity [85,86]. Thymidine–ruthenium compounds J, K [87] and L [74] exhibited interesting cancer cell toxicity with cellular uptake independent of nucleoside transporters mediation.

Trithiolato-bridged dinuclear ruthenium(II)-arene complexes (e.g., compounds M–O in Figure 1) are highly active against cancer cells but show limited selectivity [88]. Recent studies revealed that they also exhibit remarkable antiparasitic activity but also interesting selectivity profiles against *Toxoplasma gondii*, *Neospora caninum*, and *Trypanosoma brucei* [89–91]. For instance, complex O had very low IC<sub>50</sub> values of 1.2 nM for *T. gondii* and 1 nM for *N. caninum* [89,90].

Trithiolato diruthenium compounds present a structure based on two half-sandwich ruthenium(II)-arene units bridged by three thiols, the Ru<sub>2</sub>S<sub>3</sub> unit forming a trigonal-bipyramidal framework. The straightforward synthesis and scale-up of mixed trithiolato dinuclear ruthenium complexes like complex O (Figure 1) as well as their outstanding chemical inertness make this scaffold a good substrate for functionalization. Diruthenium conjugates with short peptides [92], coumarins [93], BODIPYs [94], and anticancer and antimicrobial drugs [95,96] have been reported and some of them exhibited improved water solubility, as well as enhanced anticancer or antiparasitic activity.

Amide or ester coupling reactions allowed easy modification of mixed trithiolato diruthenium compounds bearing hydroxy, amine, and carboxylic acid groups [93,95,96]. However, as in some cases this type of reaction presented shortcomings [96], other alternatives were envisioned.

The aim of this study was to generate novel hybrid molecules as improved antiparasitic compounds by exploiting the *T. gondii* auxotrophies for nucleic bases. To this end, the synthesis and biological activity assessment of new conjugates nucleobase–trithiolato-bridged dinuclear ruthenium(II)-arene unit were performed. The pool of nucleobases comprised adenine, uracil, cytosine, thymine, and xanthine. Conjugates with other types of small molecules were also synthesized and assessed to ascertain this approach.

Besides the nature of the nucleobase, the influence of the type and length of the linkers between the two moieties were also evaluated. In general, amide or ester coupling reactions allowed easy modification of mixed trithiolato diruthenium compounds bearing hydroxy, amine, and carboxylic acid groups [93,95,96]. However, as in some cases this type of reaction presented shortcomings [96], another objective of this study was to identify and validate new synthetic routes affording hybrids based on the diruthenium unit. The proposed strategy challenged the use of CuAAC reactions [97,98] with the formation of triazole connectors. Azide-alkyne click reactions proved a valuable way for the post-functionalization of metal complexes [81,99–109], whereas the triazole linkers exhibit favorable properties, including a moderate dipole character, hydrogen-bonding capability, rigidity, and stability [110]. Since click reactions require azide and alkyne partners, the use of the trithiolato diruthenium scaffold in either role can be examined in reactions with compounds containing the respective complementary group. A first example of a trithiolato–diruthenium conjugate with metronidazole obtained using a CuAAC reaction was recently reported [96].

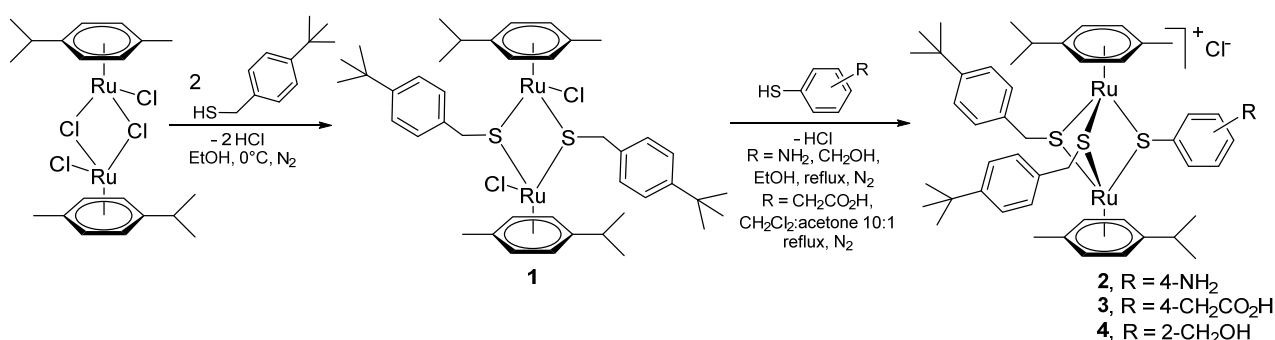
Using compound concentrations of 0.1 and 1 µM, the newly obtained hybrids and associated intermediates were submitted to a first in vitro screening, against a transgenic *T. gondii* strain constitutively expressing β-galactosidase (*T. gondii* β-gal) grown in human foreskin fibroblasts (HFF), while their cytotoxicity was evaluated in non-infected HFF by alamarBlue assay. The compounds which at 1 µM exhibited interesting antiparasitic activity (90% tachyzoite proliferation inhibition) and low cytotoxicity (>50% HFF viability), were subjected to a *T. gondii* IC<sub>50</sub> (half-maximal inhibitory concentration) determination, and HFF cytotoxicity assessment at 2.5 µM.

## 2. Results

### 2.1. Synthesis

#### 2.1.1. Synthesis of the Trithiolato-Bridged Dinuclear Ruthenium(II)-Arene Intermediates 2–9

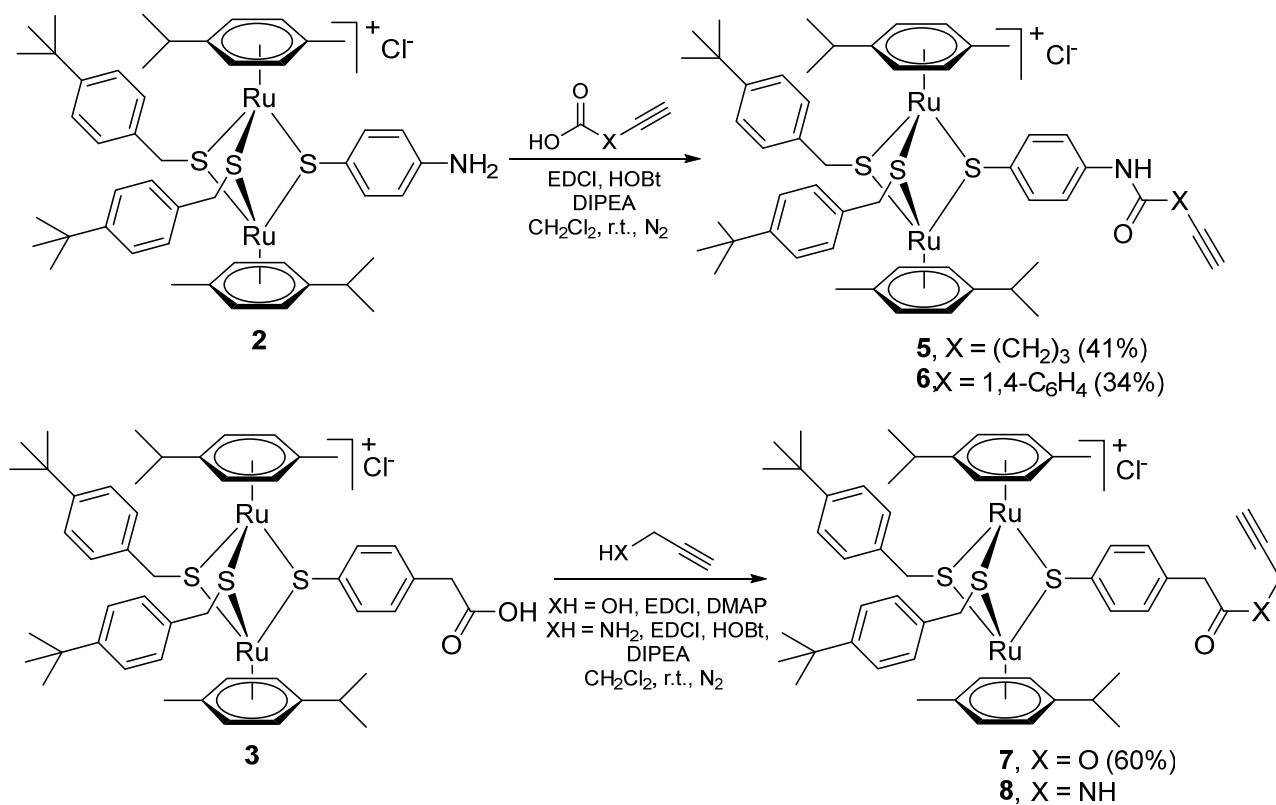
To access the hybrid molecules, nine diruthenium intermediates **2–9** bearing functional groups enabling covalent tethering (i.e., via ester conjugation or click chemistry) of appropriately substituted compounds were first synthesized. Intermediates **2–4** functionalized with an amino, carboxy, or hydroxy group, respectively, were obtained following a two-step pathway (Scheme 1) using formerly reported procedures [93,111]. Precursor **1**, obtained from the ruthenium dimer ( $[\text{Ru}(\eta^6\text{-}p\text{-MeC}_6\text{H}_4\text{Pr}^i)\text{Cl}_2]_2$ ) and (4-(*tert*-butyl)phenyl)methanethiol [93], was reacted with 4-amino-benzenethiol, 2-(4-mercaptophenyl)acetic acid and, respectively, (2-mercaptophenyl)methanol in the appropriate solvent to yield compounds **2–4**.



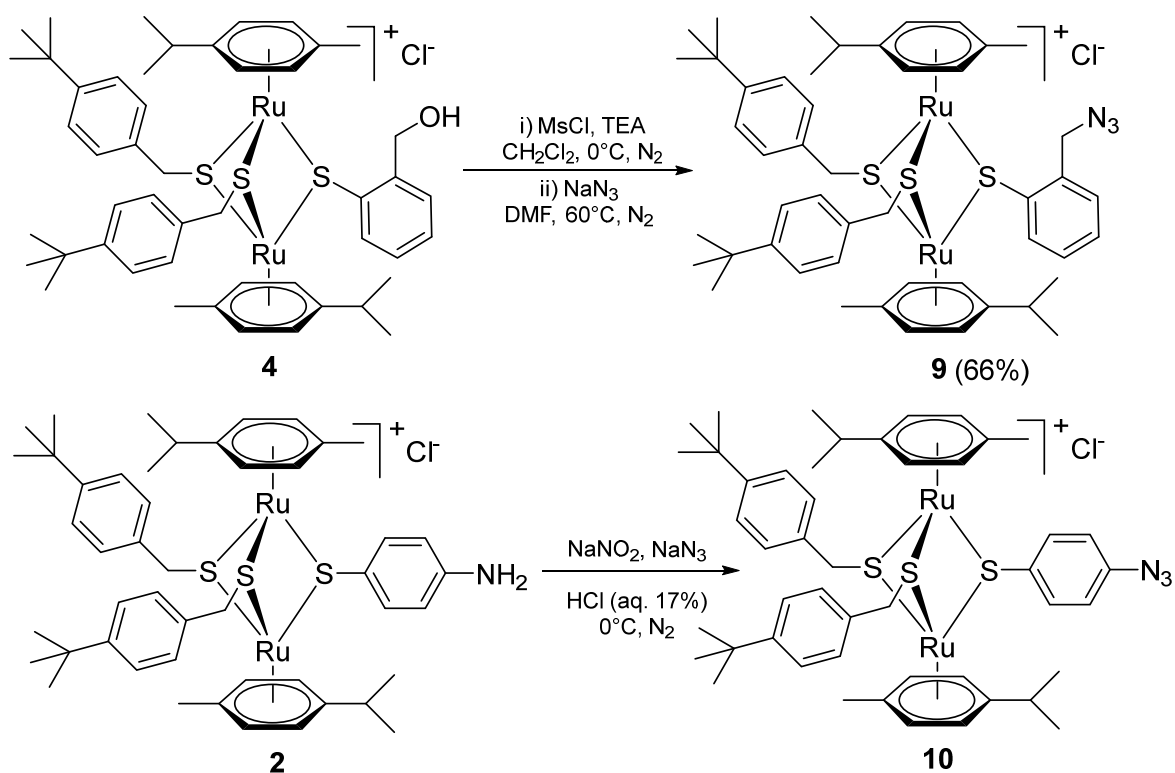
**Scheme 1.** Synthesis of the mixed dinuclear ruthenium(II)–arene intermediates **2**, **3**, and **4**.

Intermediates **2** and **3** were further reacted with various alkyne derivatives bearing carboxy, hydroxy, and amino groups using ester or amide coupling reactions as presented in Scheme 2. Reactions of amino derivative **2** with 5-hexynoic acid and 4-ethynylbenzoic acid (Scheme 2, top) in the presence of EDCI (N-(3-dimethylaminopropyl)-N'-ethylcarbodiimide hydrochloride) and HOBt (1-hydroxybenzotriazol) as coupling agents, in basic conditions (DIPEA, N,N-diisopropylethylamine), afforded the ruthenium–alkyne compounds **5** and **6** in 41 and 34% yield, respectively. Alkyne derivatives **7** and **8** were synthesized by reacting carboxy diruthenium compound **3** with propargyl alcohol and propargyl amine (Scheme 2, bottom). Ester **7** was obtained in the presence of EDCI as coupling agent and DMAP (4-(dimethylamino)pyridine) as basic catalyst and was isolated in 60% yield, while amide **8** was described previously [96].

The trithiolato diruthenium(II)–arene compounds can also function as an azide partner in click reactions. With this aim, azide-functionalized compound **9** was synthesized following a two-step process (Scheme 3 (top)). The hydroxy group of **4** was activated by mesylation with MsCl in basic conditions (TEA, triethylamine), followed by the nucleophilic substitution with azide ( $\text{NaN}_3$ ); **9** was isolated in 66% yield over two steps.



**Scheme 2.** Synthesis of the alkyne diruthenium derivatives **5–8** starting from the amino and carboxy intermediates **2** and **3**.

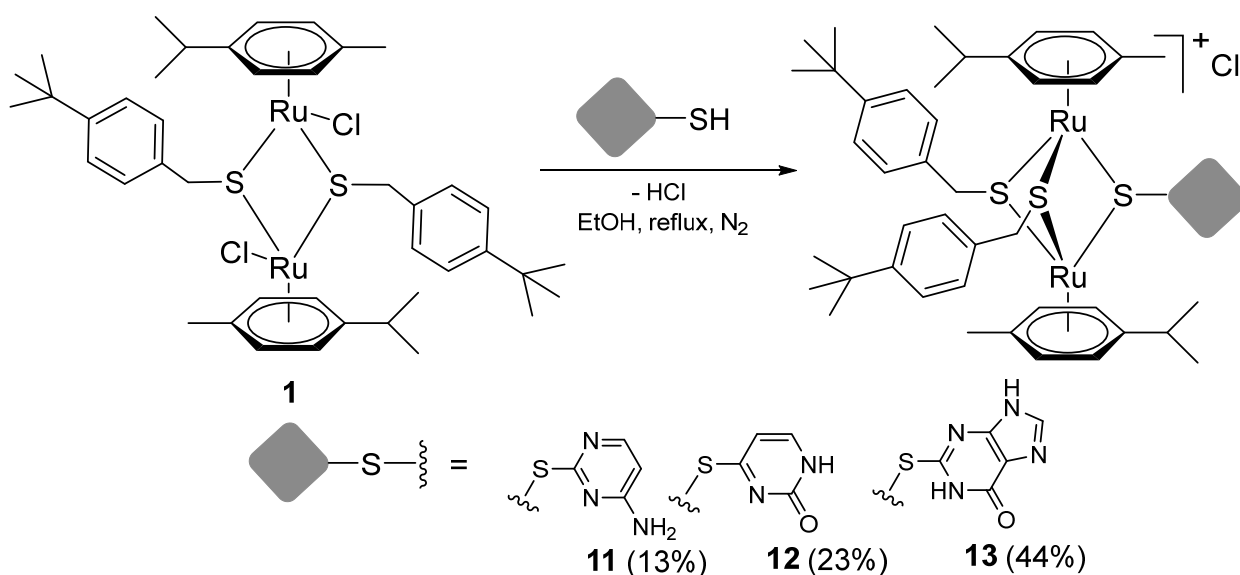


**Scheme 3.** Synthesis of the azide-diruthenium compounds **9** (top) and **10** (bottom).

Diruthenium azide **10** (Scheme 3 (bottom)) was obtained by adapting a literature procedure [112], starting from amino derivative **2** using the Sandmeyer reaction. The poor solubility of amine **2** and of the intermediate diazonium salt (not isolated) led to incomplete conversion. Compound **10** was unstable to mild heating and silicagel chromatographic purifications, and only a small quantity of this intermediate was purified for biological evaluation tests. Nevertheless, azide **10** could be used for click reactions even if it contained traces of **2**. Attempts to synthesize **10** using other literature protocols [113,114] were unsuccessful (either the azide was not obtained, or the conversion was lower). Based on their structural features, the various diruthenium conjugates obtained in this study were organized in five families.

### 2.1.2. Synthesis of Compounds 11–13 (Family 1)

In the compounds constituting family 1, the nucleobase moiety was introduced as one of the bridging thiols (Scheme 4). Reactions of the dithiolato diruthenium intermediate **1** with 2-thiocytosine, 4-thiouracil, and 2-thioxanthine afforded the mixed trithiolato derivatives **11**, **12**, and **13** in low yields of 13, 23, and 44%, respectively.

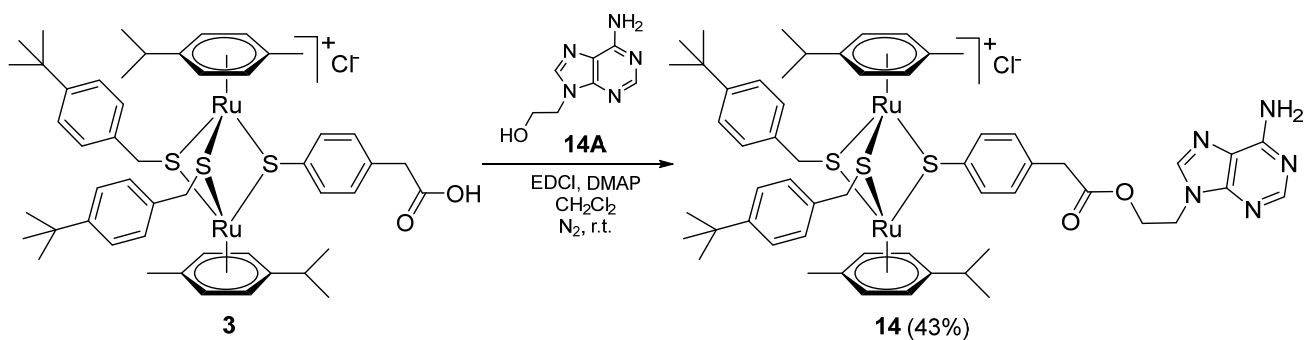


**Scheme 4.** Synthesis of the mixed trithiolato diruthenium complexes **11**, **12**, and **13**.

The introduction of nucleobase units on the trithiolato diruthenium scaffold using this method presented important limitations. In reactions run with other substrates such as 6-thioguanine, 8-mercaptoadenine, and 2-thiobarbituric acid, the reduced solubility of the thiols in refluxing EtOH led to poor conversions and important difficulties in the recovery of the pure product. Compounds **11** and **12** still contained traces of impurities and their biological activity was not assessed.

### 2.1.3. Synthesis of Compound 14 (Family 2)

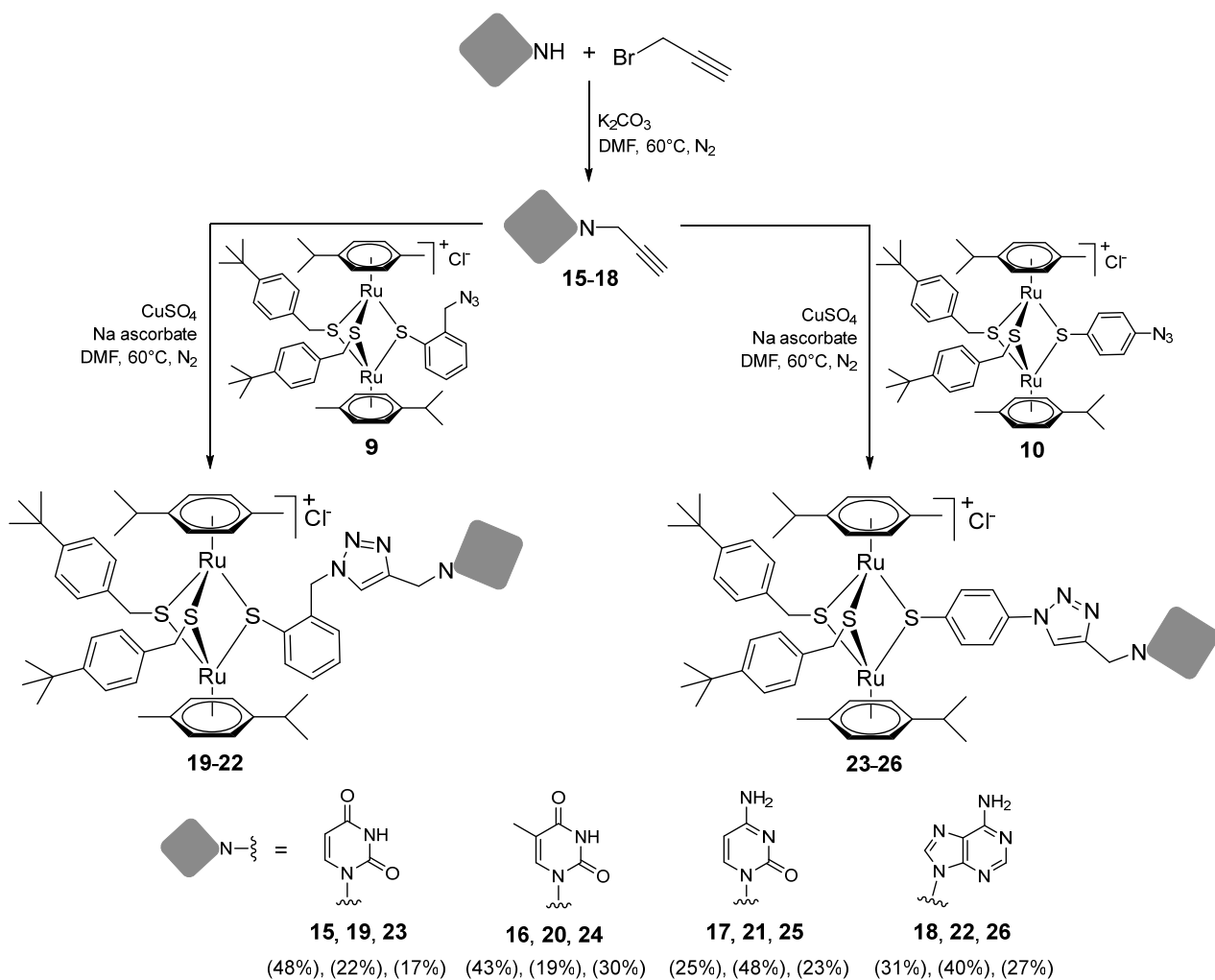
Family 2 comprises ester conjugate **14** obtained by the reaction of carboxy intermediate **3** with 9-(2-hydroxyethyl)adenine **14A** in the presence of EDCI as coupling agent and DMAP as base and was isolated in 43% yield (Scheme 5).



**Scheme 5.** Synthesis of the adenine ester conjugate **14**.

#### 2.1.4. Synthesis of Compounds **15–26** (Family 3)

The use of the click CuAAC (copper catalyzed azide–alkyne cycloaddition) reactions [101,115] for the obtainment of new conjugates with nucleobases was challenged. A first series of reactions were run using diruthenium azide derivatives **9** and **10** as substrates (Scheme 6).



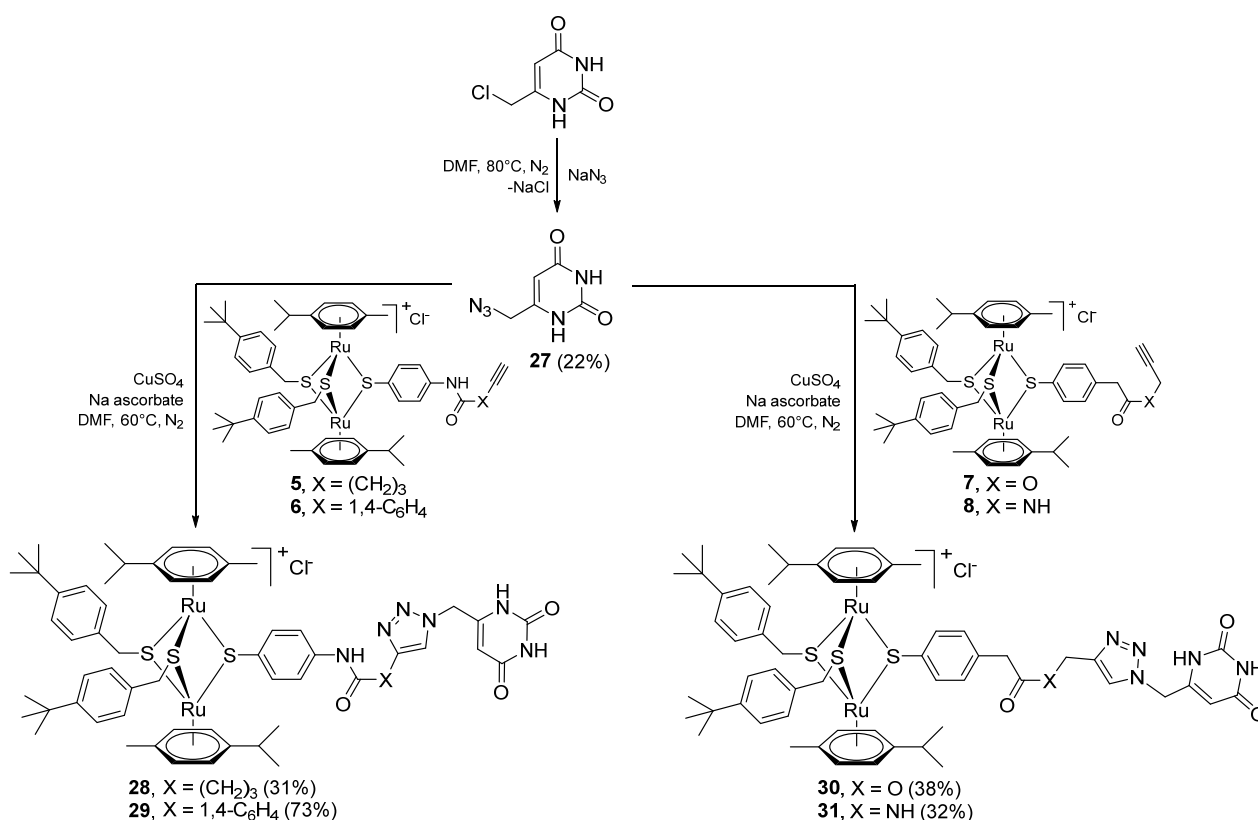
**Scheme 6.** Synthesis of the uracil (**15**), thymine (**16**), cytosine (**17**), and adenine (**18**) propargyl derivatives and their CuAAC reactions with the diruthenium azides **9** (left) and **10** (right), affording conjugates **19–22** and, respectively, **23–26**.

*N*-Propargyl derivatives of uracil (**15**), thymine (**16**), cytosine (**17**), and adenine (**18**) were synthesized by the nucleophilic substitution reactions performed on propargyl bromide with the corresponding nucleobases in basic conditions ( $K_2CO_3$ ), by adapting literature procedures [116–118] (Scheme 6). Alkyne derivatives **15–18** were isolated in low to medium yields (25–48% range). The synthesis of the nucleobase propargyl derivatives **15–18** using either directly the nucleobases or appropriately protected intermediates was previously reported [119–121]. In this study, the synthesis of derivatives **15–18** was not optimized as our purpose was to obtain these intermediates in the quantity and quality allowing the click reactions and the *in vitro* biological activity screening. The  $^1H$  and  $^{13}C$  NMR data for compounds **15–18** (Supplementary Materials) are in good agreement with the published data [122–124], taking the different conditions used for the measurements.

The CuAAC reactions were performed by adapting reported protocols [101,115], in the presence of  $CuSO_4$  as catalyst and sodium ascorbate as reducing agent. Nucleobase propargyl derivatives **15–18** were reacted with azides **9** and **10** (Scheme 6), affording the click products **19–22** and **23–26** in low yield (19–48% and 17–30% range, correspondingly). The quantities of isolated products were suitable for a first antiparasitic activity and cytotoxicity screening.

#### 2.1.5. Synthesis of Compounds 27–33 (Family 4)

The diruthenium complexes can act as alkyne partner in CuAAC reactions. As azide component, 6-(azidomethyl)uracil **27** was synthesized (isolated 22% yield) by the nucleophilic substitution of the chlorine in 6-(chloromethyl)uracil with  $NaN_3$  (Scheme 7).

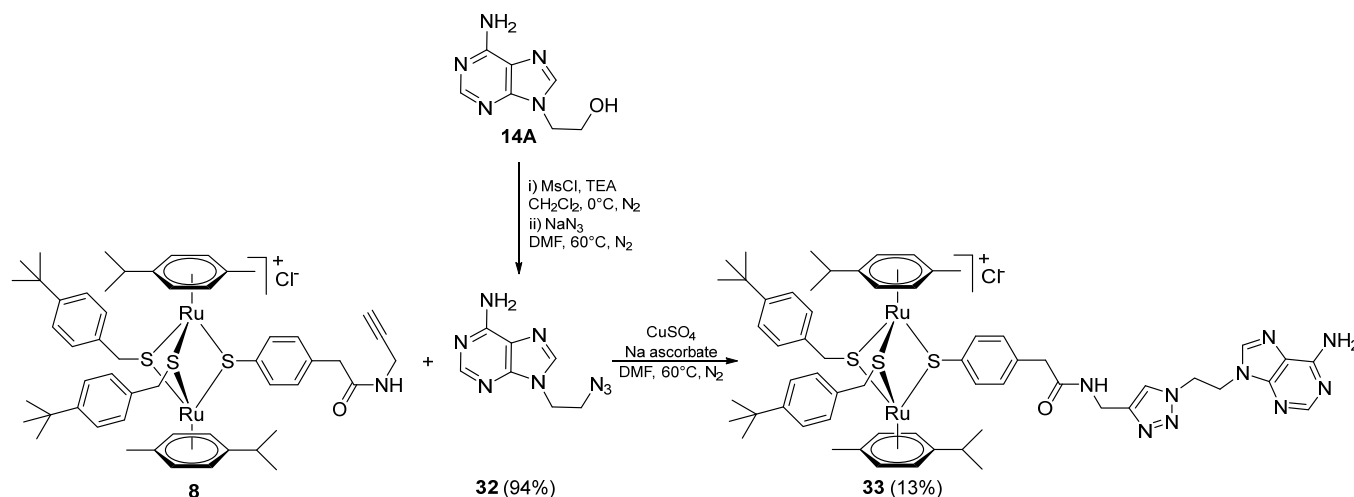


**Scheme 7.** Synthesis of the azide uracil derivative **27** and of the corresponding click conjugates **28–31**, using diruthenium alkyne derivatives **5–8**.

The uracil azide **27** was reacted with the alkyne functionalized diruthenium derivatives **5–8** (Scheme 7) in the presence of  $CuSO_4$  and sodium ascorbate [101,115], affording the corresponding click products **28–31** in low to medium yields (31 to 73% range). These

reactions afforded conjugates presenting two types of spacers (aliphatic **28** vs. aromatic **29**) and having ester (**30**) or amide bonds in the linking units (**28**, **29**, and **31**) (Scheme 7).

Adenine azide derivative **32** was synthesized in two steps starting from 9-(2-hydroxyethyl)adenine (**14A**) and was reacted with the alkyne functionalized diruthenium compound **8**, to afford conjugate **33** in 13% yield (Scheme 8).



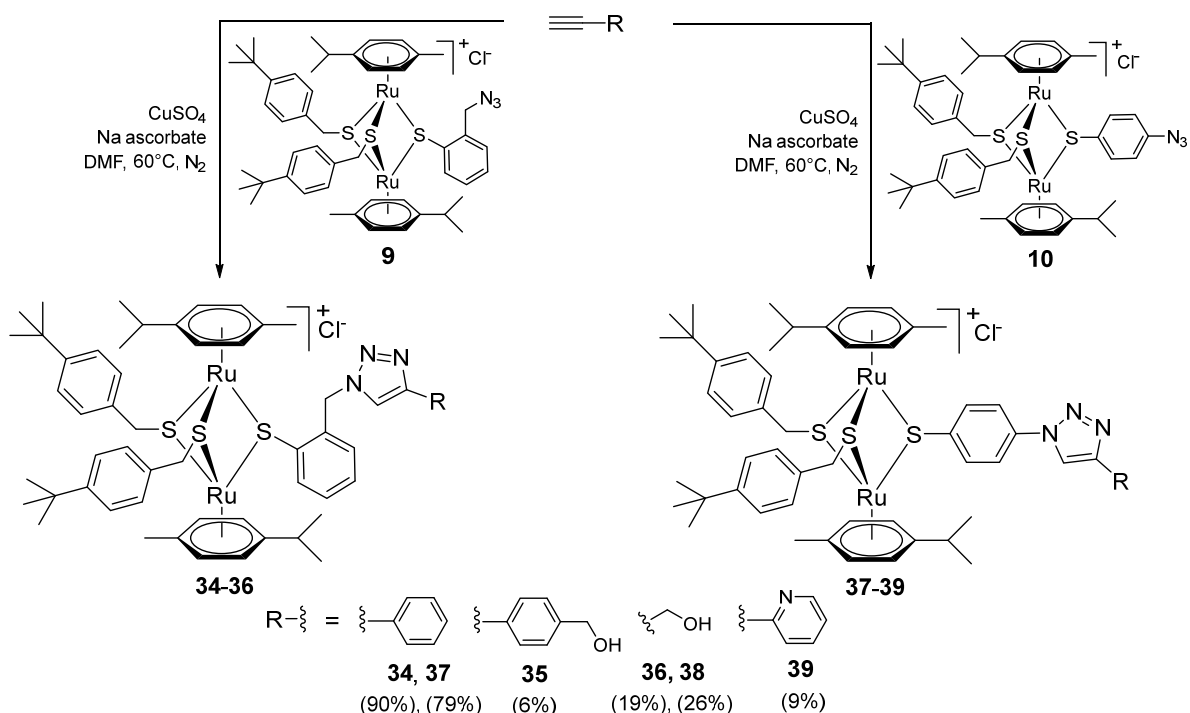
**Scheme 8.** Synthesis of the azide adenine derivative **32** and of the corresponding click conjugate **33**.

#### 2.1.6. Synthesis of Compounds **34–39** (Family 5)

To evaluate the impact of the nature of the substituent anchored on the diruthenium scaffold on the biological activity, click conjugates of azides **9** and **10** with various alkyne derivatives such as ethynylbenzene, 4-ethynylbenzyl alcohol, propargyl alcohol, and 2-ethynylpyridine were also synthesized (Scheme 9), the reactions being performed in similar conditions [101,115].

If the phenyl derivative **34** was obtained in good yield (90%), the products with polar substituents were isolated only in poor yields (6% for **35** and 19% for **36**). A similar effect was observed in the reactions run with azide **10**, as the phenyl click product **37** was isolated in high yield (79%), while the reactions with more polar ethynyl compounds were less performant affording compounds **38** and **39** only in 26 and, respectively, 9% yield. The alkyne reactivity can increase as the para-substituent becomes more electron-withdrawing, resulting in acidic  $\text{C}_{\text{sp}}\text{-H}$  bonds [122]. The conversion seems to be influenced also by polar effects not only by substituent electronic properties. This can explain the higher yield obtained with lipophilic phenylacetylene compared to more polar propargyl alcohol and 4-ethynylbenzyl alcohol. Note that the syntheses were not optimized as the aim was to obtain the click compounds satisfying the quantity and quality requirements necessary for a first in vitro bioactivity screening. The reported yields correspond to the isolated pure compounds and do not always reflect the conversion, as the purification of some compounds was more laborious.

All compounds were fully characterized by  $^1\text{H}$  and  $^{13}\text{C}$  NMR (Nuclear Magnetic Resonance) spectroscopy, ESI-MS (electrospray ionization mass spectrometry) and elemental analysis experiments (the full description is presented in the Supporting information).



**Scheme 9.** CuAAC reactions of azide diruthenium derivatives **9** (left) and **10** (right) with ethynylbenzene, 4-ethynylbenzyl alcohol, propargyl alcohol, and 2-ethynylpyridine.

#### 2.1.7. Stability of the Compounds

For the biological activity evaluation, 1 mM stock solutions of all compounds were prepared in dimethylsulfoxide (DMSO).  $^1\text{H}$ -NMR spectra of intermediate **4** and of conjugates **24**, **28**, **33**, and **39** in DMSO- $d_6$ , recorded at  $25^\circ\text{C}$  5 min and 100 days after sample preparation, showed no modifications (see Supporting information), demonstrating very good stability of the diruthenium compounds in this highly complexing solvent.

Furthermore, for evaluating the compounds' potential nucleobase-pairing via H-bonding interactions,  $^1\text{H}$ -NMR measurements were performed using DMSO- $d_6$  solutions of uracil, thymine, cytosine, and adenine conjugates **23**, **24**, **25**, and **26** and of the respective complementary nucleic bases (see details in Supporting information). These experiments further evidenced the stability of the diruthenium–nucleobase conjugates in DMSO- $d_6$ . The presence of weak H-bonding interactions between the conjugates and the nucleobases was demonstrated by the broadening and the small chemical shift changes of the resonance signals corresponding to the NH groups (Figures S3–S7).

Compounds **7**, **14**, and **30** have an ester linker that can potentially be hydrolyzed in growth media. Comparable conjugates with coumarin and BODIPY fluorescent units linked through ester bonds to the diruthenium unit were recently investigated [93,94]. As a very limited solvolysis of the ester bonds was noticed after 168 h for some compounds, it was concluded that the coumarin and BODIPY diruthenium conjugates exhibit high stability in the conditions used for the biological evaluations [93]. Therefore, it was assumed that compounds **7**, **14**, and **30** are sufficiently stable for the in vitro evaluation.

### 2.2. Assessment of the In Vitro Activity against *T. gondii* $\beta$ -gal and Host Cells

#### 2.2.1. Primary Screening

The compounds (conjugates and respective intermediates) were subjected to a sequential biological screening. The antiparasitic activity (proliferation inhibition) was evaluated using *T. gondii*  $\beta$ -gal grown in HFF host cell monolayers and the cytotoxic effects were studied in non-infected HFF monolayers [90]. A first screening (Table 1 and Figure 2) of all compounds against *T. gondii*  $\beta$ -gal tachyzoites and HFF was carried out at concentrations

of 0.1 and 1  $\mu\text{M}$ . In a second screening, the selected compounds (which at 1  $\mu\text{M}$  inhibited *T. gondii*- $\beta$ -gal proliferation by at least 90% and impaired the HFF viability not more than 50%) were submitted to dose-response studies to determine the  $\text{IC}_{50}$  values, while cytotoxicity in HFF was assessed at 2.5  $\mu\text{M}$  (the results are summarized in Table 2). The same screening strategy was applied in previous studies [111]. Pyrimethamine ( $\text{IC}_{50} = 0.326 \mu\text{M}$ ) was used as reference compound as shown earlier [93].

**Table 1.** Primary cytotoxicity/efficacy screening of all compounds in non-infected HFF cultures and *T. gondii*  $\beta$ -gal tachyzoites cultured in HFF. Tests were performed in triplicate. The 20 compounds selected for the dose-response study against *T. gondii*  $\beta$ -gal and the assessment of the toxicity against HFF are highlighted in bold.

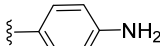
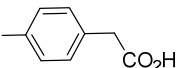
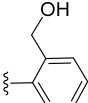
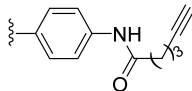
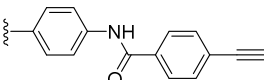
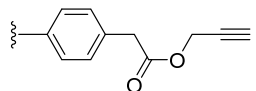
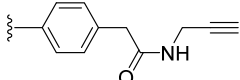
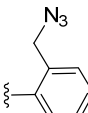
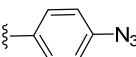
Compound	R	HFF Viability (%)		<i>T. gondii</i> $\beta$ -gal Growth (%)	
		0.1 $\mu$ M	1 $\mu$ M	0.1 $\mu$ M	1 $\mu$ M
Diruthenium intermediates					
2 <sup>a</sup>		74 $\pm$ 2	48 $\pm$ 1	57 $\pm$ 1	2 $\pm$ 0
3 <sup>a</sup>		91 $\pm$ 4	73 $\pm$ 1	114 $\pm$ 2	110 $\pm$ 2
4 <sup>a</sup>		80 $\pm$ 1	69 $\pm$ 6	2 $\pm$ 0	1 $\pm$ 0
5		101 $\pm$ 0	96 $\pm$ 0	21 $\pm$ 2	0 $\pm$ 0
6		95 $\pm$ 1	49 $\pm$ 2	112 $\pm$ 1	6 $\pm$ 1
7		100 $\pm$ 2	53 $\pm$ 3	19 $\pm$ 1	0 $\pm$ 0
8 <sup>a</sup>		71 $\pm$ 2	46 $\pm$ 6	52 $\pm$ 13	3 $\pm$ 1
9		96 $\pm$ 1	64 $\pm$ 1	9 $\pm$ 1	1 $\pm$ 1
10		94 $\pm$ 1	70 $\pm$ 1	10 $\pm$ 0	1 $\pm$ 0

Table 1. Cont.

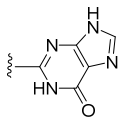
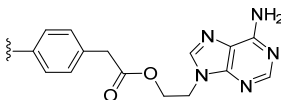
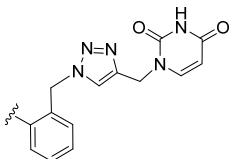
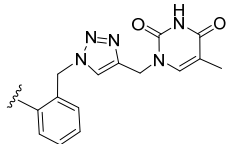
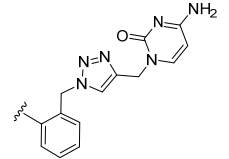
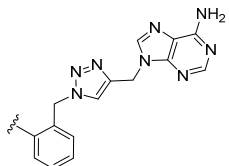
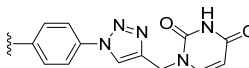
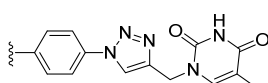
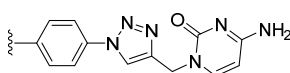
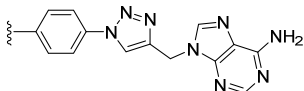
Compound	R	HFF Viability (%)		<i>T. gondii</i> β-gal Growth (%)	
		0.1 μM	1 μM	0.1 μM	1 μM
Family 1					
13		156 ± 1	102 ± 1	85 ± 2	83 ± 2
Family 2					
14		95 ± 11	76 ± 2	12 ± 1	1 ± 0
Family 3					
19		93 ± 2	85 ± 0	117 ± 7	7 ± 0
20		100 ± 2	71 ± 2	102 ± 0	1 ± 0
21		109 ± 2	89 ± 1	4 ± 0	0 ± 0
22		102 ± 0	77 ± 2	79 ± 3	1 ± 0
23		100 ± 1	76 ± 1	114 ± 4	1 ± 0
24		98 ± 10	96 ± 4	56 ± 15	0 ± 0
25		94 ± 9	91 ± 8	82 ± 6	35 ± 7
26		109 ± 2	76 ± 0	109 ± 6	0 ± 0

Table 1. Cont.

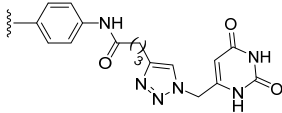
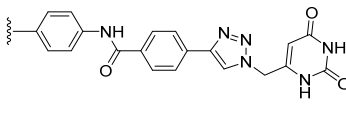
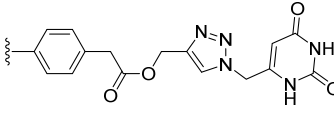
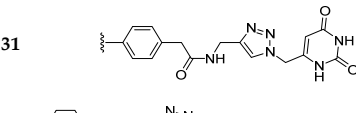
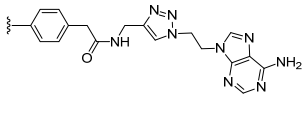
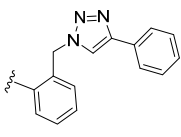
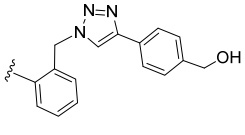
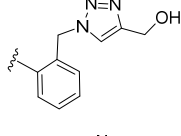
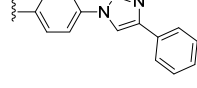
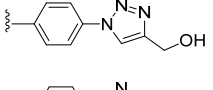
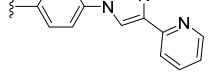
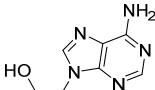
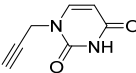
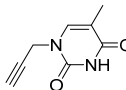
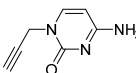
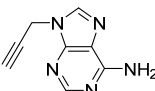
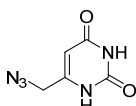
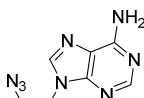
Compound	R	HFF Viability (%)		<i>T. gondii</i> $\beta$ -gal Growth (%)	
		0.1 $\mu$ M	1 $\mu$ M	0.1 $\mu$ M	1 $\mu$ M
Family 4					
28		101 $\pm$ 1	88 $\pm$ 1	97 $\pm$ 6	76 $\pm$ 5
29		101 $\pm$ 1	102 $\pm$ 1	102 $\pm$ 3	116 $\pm$ 5
30		114 $\pm$ 0	112 $\pm$ 3	142 $\pm$ 3	7 $\pm$ 0
31	31 	99 $\pm$ 3	98 $\pm$ 6	109 $\pm$ 0	127 $\pm$ 0
33		84 $\pm$ 6	71 $\pm$ 3	94 $\pm$ 11	83 $\pm$ 11
Family 5					
34		96 $\pm$ 1	70 $\pm$ 1	7 $\pm$ 0	1 $\pm$ 0
35		89 $\pm$ 0	27 $\pm$ 1	1 $\pm$ 0	0 $\pm$ 0
36		115 $\pm$ 1	87 $\pm$ 2	7 $\pm$ 0	0 $\pm$ 0
37		99 $\pm$ 1	71 $\pm$ 0	13 $\pm$ 1	0 $\pm$ 0
38		104 $\pm$ 1	71 $\pm$ 1	42 $\pm$ 2	0 $\pm$ 0
39		94 $\pm$ 2	90 $\pm$ 1	14 $\pm$ 1	0 $\pm$ 0

Table 1. Cont.

Compound	R	HFF Viability (%)		<i>T. gondii</i> β-gal Growth (%)	
		0.1 μM	1 μM	0.1 μM	1 μM
Nucleobase intermediates					
14A		136 ± 3	84 ± 14	104 ± 2	75 ± 11
15		107 ± 2	96 ± 2	109 ± 5	83 ± 0
16		104 ± 2	103 ± 3	96 ± 8	95 ± 6
17		96 ± 1	93 ± 1	111 ± 5	90 ± 7
18		96 ± 2	89 ± 3	117 ± 4	91 ± 6
27		98 ± 5	102 ± 3	101 ± 5	99 ± 11
32		104 ± 2	103 ± 3	103 ± 8	94 ± 2

<sup>a</sup> The antiparasitic activity and the cytotoxicity of intermediated 2–4 was discussed formerly [93,111]. % indicates viability of HFF or proliferation of *T. gondii*  $\beta$ -gal tachyzoites in relation to untreated controls.

The antiparasitic activity of compounds 2–4 and 8 was previously reported and discussed [93,96,111] and the values are provided in Table 1 and Figure 2 for comparison.

From the diruthenium alkyne intermediates 5–8, only derivative 5 presented reduced toxicity on HFF at 1  $\mu$ M, while amide 8 affected HFF viability even at 0.1  $\mu$ M. Compound 5 exhibited an improved antiparasitic efficacy compared to its amino diruthenium precursor 2. Ester 7 and amide 8 affected more the proliferation of *T. gondii*  $\beta$ -gal than the carboxy precursor 3 but also exerted a stronger effect on the host cells viability at 1  $\mu$ M. Both diruthenium azides 9 and 10 exhibited high activity against the parasite even at 0.1  $\mu$ M and were moderately toxic to HFF at 1  $\mu$ M.

The nucleic base intermediates 14A, 15–18, 27, and 32 were non-toxic to the host cells and exhibited no antiparasitic activity against *T. gondii*  $\beta$ -gal at 1  $\mu$ M.

In family 1, compound 13, with 2-thioxanthine as one of the thiol bridges, neither affected HFF viability, nor was active against the parasite at both tested concentrations.

The adenine ester conjugate 14 from family 2 exhibited significantly improved antiparasitic activity compared to its precursors 3 and 14A (9-(2-hydroxyethyl) adenine), almost abolishing parasite proliferation at 1  $\mu$ M, while exhibiting moderate HFF toxicity at the same concentration.

From the compounds of family 3, the uracil, thymine, cytosine, and adenine click conjugates 19–22 were moderately toxic when tested at 1  $\mu$ M. Nucleobase hybrids 19–22 almost abolished parasite proliferation at 1  $\mu$ M, but only the cytosine conjugate 21 exhibited a strong antiparasitic effect at 0.1  $\mu$ M.

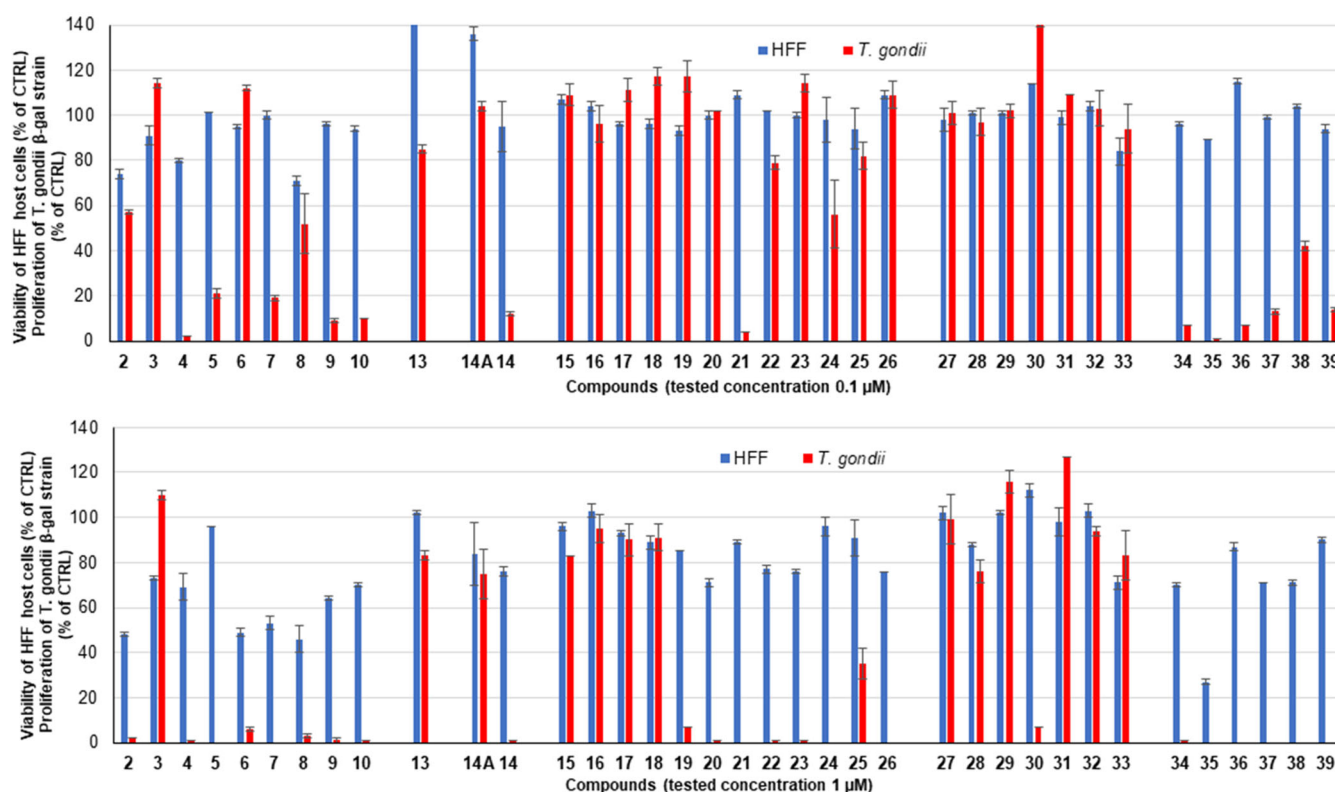


**Figure 2.** Clustered column chart showing the in vitro activities at 0.1 (top) and 1 μM (bottom) of the tested compounds on HFF viability and *T. gondii* β-gal proliferation. Non-infected HFF monolayers treated only with 0.1% DMSO exhibited 100% viability and 100% proliferation was attributed to *T. gondii* β-gal tachyzoites treated only with 0.1% DMSO. For each assay, standard deviations were calculated from triplicates and are displayed on the graph. Data for compounds 2–4 and 8 were previously reported [79,82,97].

Compounds 23–26 did not affect HFF viability at 0.1 μM, but the uracil and adenine derivatives 23 and 26 presented moderate toxicity to the host cells at 1 μM (HFF viability 76% for both). Among compounds 23–26, the thymine functionalized compound 24 had a stronger antiparasitic effect at 0.1 μM, while cytosine derivative 25 had a low effect on parasite proliferation even at 1 μM. Conjugates 23, 24, and 26, bearing uracil, thymine, and adenine, almost abolished parasite proliferation when applied at 1 μM. Overall, compared to the diruthenium azide precursor 10, nucleobase click conjugates 23–26 applied at 1 μM affected HFF to a lower degree, but exhibited reduced antiparasitic activity at 0.1 μM.

When comparing conjugates presenting the same nucleobase in family 3, cytosine derivatives 21 and 25 exhibited the most striking differences in *T. gondii* β-gal activity. While 21 almost abolished parasite proliferation when applied at 0.1 μM (4%), 25 exerted reduced antiparasitic efficacy even at 1 μM (35%). This suggests that both the linking mode and the type of nucleobase influence the activity of the conjugates.

In family 4, the uracil triazole conjugates 28–31 were non-toxic to HFF at 1 μM. However, among their respective diruthenium alkyne intermediates, only 5 did not affect HFF viability at 1 μM, while 6, 7, and 8 were toxic to the host cells at the same concentration. Analogues 28, 29, and 31, with amide bonds in their linking unit, presented reduced to no efficacy against *T. gondii* β-gal even at 1 μM. However, compound 30, with an ester bond in the connecting part, presented a significantly stronger antiparasitic effect compared to amide 31 when applied at 1 μM. Related to uracil derivative 31, adenine functionalized compound 33 presented a slightly increased activity against the parasite but also higher cytotoxicity to host cells.

In family 5, toxicity differences were observed between click compounds **34–36** obtained from the diruthenium azide derivative **9**. Compound **35** showed important HFF toxicity at 1  $\mu\text{M}$ , while derivative **36** was highly active against the parasite at 0.1  $\mu\text{M}$  and was non-toxic to the host cells even at 1  $\mu\text{M}$ . Interestingly, phenyl derivative **37** presented a similar toxicity profile to its analogue **34** with a different mode of linking to the diruthenium moiety. For compounds presenting the methylene-hydroxy group as substituent, **38** exhibited slightly increased HFF toxicity and a reduced antiparasitic efficacy when applied at 0.1  $\mu\text{M}$  compared to **36**. In family 5, compared to precursor diruthenium azides **9** and **10**, only click products **36** and **39** exhibited an improved HFF toxicity/parasite efficacy profile.

Comparing adenine conjugates **14**, **22**, and **26**, the most promising candidate for further studies is the ester analogue **14**. The uracil hybrids **19**, **23**, **28**, **29**, **30**, and **31** exhibited reduced toxicity to HFF at 1  $\mu\text{M}$  but also limited activity against the parasite at 0.1  $\mu\text{M}$ . Compounds **19**, **23**, and **30** presented antiparasitic properties only at 1  $\mu\text{M}$ , while **28**, **29**, and **31** showed low antiparasitic activity even at this concentration.

#### 2.2.2. $\text{IC}_{50}$ Values against *T. gondii* $\beta$ -Gal Tachyzoites and HFF Toxicity at 2.5 $\mu\text{M}$

In a secondary screening, the dose-response studies ( $\text{IC}_{50}$  values) against *T. gondii*  $\beta$ -gal tachyzoites and the HFF toxicity at 2.5  $\mu\text{M}$  for 20 selected compounds (which, when applied at 1  $\mu\text{M}$ , inhibited *T. gondii*- $\beta$ -gal proliferation by at least 90% and did not alter HFF viability by more than 50%) were determined (the results are summarized in Table 2). The same screening strategy was applied in previous studies [111].

Among the diruthenium intermediates, carboxy derivative **3** did not affect HFF viability, amine **2** and propargyl ester **7** exhibited medium toxicity on HFF at 2.5  $\mu\text{M}$  (51% for both), and all the other compounds were highly cytotoxic.

The adenine ester derivative **14** from family 2 was very promising with an  $\text{IC}_{50}$  value of 0.059  $\mu\text{M}$  (5 times lower than that of the standard drug pyrimethamine,  $\text{IC}_{50}$  = 0.326  $\mu\text{M}$ ), and with moderate effect on HFF cells (76% viability at 2.5  $\mu\text{M}$ , a concentration 40 times higher compared to its  $\text{IC}_{50}$ ). Of note, compound **14** exhibited significantly improved antiparasitic activity compared to its diruthenium precursor **3**, with a low increase of host cells cytotoxicity [111].

From family 3, only click conjugates **19**, **22**, **23**, and **24** presented medium or low toxicity on the host cells. Adenine compound **22** exhibited a promising  $\text{IC}_{50}$  value of 0.108  $\mu\text{M}$ , but also considerably impaired HFF viability (52%). Uracil and thymine click derivatives **23** and **24** had a lower impact on the host cells viability (64 and 85%) but presented  $\text{IC}_{50}$  values higher or comparable to that of pyrimethamine (0.426 and 0.357  $\mu\text{M}$ ). Interestingly, the *ortho* substituted conjugates **19–22** are on average slightly more toxic to HFF than the *para* substituted conjugates **23**, **24**, and **26**. Both uracil and thymine click derivatives **23** and **24** are less toxic to HFF than the parent diruthenium azide derivative **10**.

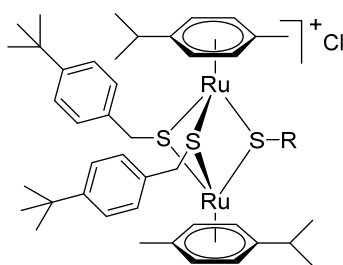
The uracil derivative **30** (click compound presenting an ester bond, family 4) did not affect host cells at 2.5  $\mu\text{M}$  (97%) but exhibited a high  $\text{IC}_{50}$  value (0.659  $\mu\text{M}$ ).

From the click products with other types of substituents (family 5), compounds **34**, **37**, and **39** were highly toxic against HFF at 2.5  $\mu\text{M}$ , and thus, anchoring hydrophobic molecules to the diruthenium scaffold via triazole units appears to be detrimental to the toxicity of HFF. The way in which the substituents are linked to the diruthenium scaffold appears to be important as the triazole-phenyl derivative **34** was significantly more toxic to the host cells compared to its analogue **37** (3 vs. 17%). The triazole-hydroxymethylene compounds **36** and **38** exhibited similar  $\text{IC}_{50}$  values on *T. gondii*  $\beta$ -gal (0.111 vs. 0.128  $\mu\text{M}$ ) for medium toxicity against HFF (77 vs. 59%). Only conjugates **36** and **38** were less toxic to the host cell compared to the parent diruthenium azide derivatives **9** and **10**.

No specific SAR (structure-activity relationships) could be identified. Both the attached unit and the connector play an important role in the biological activity. If the interactions of the anchored unit with potential biochemical targets (DNA, proteins) are indeed responsible for the observed biological activity of the conjugates, the structure of some compounds (e.g., those in which the connectors between the two units are longer and

more flexible as in conjugates **14**, **28** or **30**, **31** and **33**) could be more favorable compared to that of hybrids in which the access to the pendants is more sterically hindered (e.g., compounds **19–22**). The observed biological effects both in terms of host cell toxicity and antiparasitic activity are multifactorial, as along with the attached molecule, the connecting position, the bonds present in the linker and its rigidity, are also very important. Of note, if in the structure of the conjugates the presence of metabolites like nucleobases can favor cell accumulation, the size of the diruthenium unit could constitute a limitative factor in membrane transfer. Assessing the conjugates obtained in this study against other purine auxotrophic parasites, such as *Leishmania donovani* and *Plasmodium falciparum* [123] could further validate the proposed approach.

**Table 2.** Half maximal inhibitory concentration (IC<sub>50</sub>) values (μM) on *T. gondii* β-gal for the 20 selected compounds and their effect at 2.5 μM on HFF viability.



Compound	R	IC <sub>50</sub> (μM)	[LS; LI] <sup>c</sup>	SE <sup>d</sup>	HFF Viability (%) <sup>e</sup>	SD <sup>f</sup>
Diruthenium intermediates						
<b>4<sup>b</sup></b>		0.038	[0.060; 0.023]	0.110	4	2
<b>5</b>		0.038	[0.050; 0.029]	0.063	34	1
<b>6</b>		0.288	[0.348; 0.238]	0.188	17	1
<b>7</b>		0.289	[0.363; 0.230]	0.229	51	3
<b>9</b>		0.048	[0.058; 0.040]	0.139	11	1
<b>10</b>		0.064	[0.080; 0.051]	0.050	38	1

Table 2. Cont.

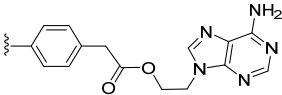
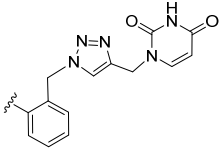
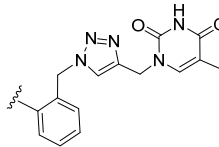
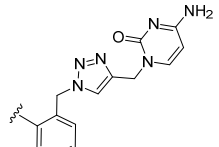
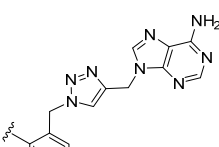
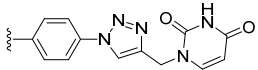
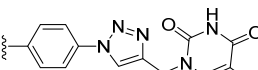
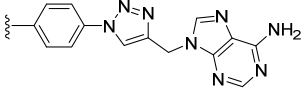
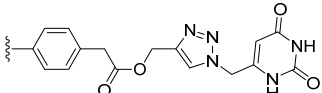
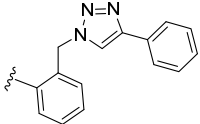
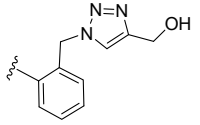
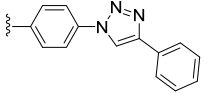
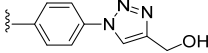
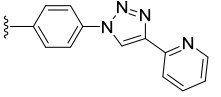
Compound	R	IC <sub>50</sub> ( $\mu$ M)	[LS; LI] <sup>c</sup>	SE <sup>d</sup>	HFF Viability (%) <sup>e</sup>	SD <sup>f</sup>
Family 2						
14		0.059	[0.085; 0.040]	0.037	76	3
Family 3						
19		0.460	[0.626; 0.338]	0.307	50	0
20		0.363	[0.371; 0.354]	0.023	39	1
21		0.046	[0.058; 0.037]	0.048	38	1
22		0.108	[0.141; 0.083]	0.066	52	1
23		0.426	[0.553; 0.328]	0.260	64	1
24		0.357	[0.418; 0.305]	0.156	85	4
26		0.178	[0.226; 0.140]	0.061	45	2
Family 4						
30		0.659	[0.684; 0.635]	0.037	97	1

Table 2. Cont.

Compound	R	IC <sub>50</sub> (μM)	[LS; LI] <sup>c</sup>	SE <sup>d</sup>	HFF Viability (%) <sup>e</sup>	SD <sup>f</sup>
Family 5						
34		0.092	[0.108; 0.078]	0.038	3	0
36		0.111	[0.135; 0.090]	0.039	77	1
37		0.096	[0.122; 0.076]	0.057	17	1
38		0.128	[0.164; 0.099]	0.058	59	1
39		0.075	[0.091; 0.061]	0.043	1	0
Pyrimethamine <sup>a</sup>		0.326	[0.396; 0.288]	0.051	99	6

<sup>a</sup> Compounds reported in Ref. [93]. <sup>b</sup> Compound reported in Ref. [96]. <sup>c</sup> Values at 95% confidence interval (CI), LS is the upper limit of CI and LI is the lower limit of CI. <sup>d</sup> The standard error of the regression (SE) represents the average distance that the observed values fall from the regression line. <sup>e</sup> Control HFF cells treated only with 0.25% DMSO exhibited 100% viability. <sup>f</sup> The standard deviation of the mean (six replicate experiments).

The most interesting compounds that deserve to be considered for further studies are ester **14** (conjugated to 9-(2-oxyethyl)adenine) and click product **36** (bearing a 2-(4-(hydroxymethyl)-1H-1,2,3-triazol-1-yl)methyl substituent). Both **14** and **36** exhibit slightly lower toxicity on HFF compared to the standard drug pyrimethamine but significantly improved antitoxoplasma activity. Adenine ester conjugate **14** exhibits improved antiparasitic properties compared to both its precursors the carboxy diruthenium compound **3** and 9-(2-hydroxyethyl)adenine (**14A**), and this type of connection should be considered for the future development of other nucleobase conjugates.

The mechanisms of action of trithiolato diruthenium compounds have not yet been elucidated. These compounds generally exhibit reduced water solubility [88] and contrary to other Ru(II)-arene complexes presenting labile chlorine or carboxylate ligands, they do not hydrolyze and are stable in the presence of most biomolecules such as amino acids and DNA [88]. Only the oxidation of cysteine (Cys) and glutathione (GSH) to form cystine and GSSG, respectively, was observed in the presence of some compounds, but no correlation between the in vitro cytotoxicity and the catalytic activity on the oxidation reaction of glutathione was observed [124,125]. Recently, inductively coupled plasma mass spectrometry (ICP-MS) experiments proved that complexes **M** and **N** (Figure 1) specifically target the mitochondrion in A2780 ovarian cancer cells [89]. Noteworthy, TEM (transmission electron microscopy) studies of different protozoan parasites (*Toxoplasma gondii*, *Neospora caninum*, *Trypanosoma brucei*) treated with trithiolato dinuclear ruthenium(II)-arene complexes revealed alterations in the mitochondrial ultrastructure pointing out this organelle as a potential target [89]. Interestingly, a similar effect was also observed in the case of trithiolato diruthenium conjugates with coumarin and BODIPY fluorophores [93,94].

The potential cellular and molecular targets of conjugate **14** were recently investigated [126]. Affinity chromatography of parasite extracts on epoxy-sepharose-bound conjugate **14**, which is also highly active against *T. brucei* bloodstream forms [126], showed that this compound interacts with mitochondrial proteins in both parasite species. In *T. gondii*, a major compound **14** binding protein is an homolog to the human mitochondrial import inner membrane translocase subunit Tim1, which is putatively involved in importing proteins from the cytoplasm into the mitochondrion. The mitochondrion as a major target of ruthenium compounds has been identified earlier in both *T. gondii* and *T. brucei*, primarily by TEM [90,91]. However, besides mitochondrial proteins, affinity chromatography has also identified a range of other binding proteins that could be assigned to different cellular pathways, which indicates that this compound could affect several important cellular functions [126]. It is conceivable that, in terms of mode of action, the adenine part of the conjugate **14** could facilitate the uptake of the ruthenium moiety, which would then be processed intracellularly and exert its antiparasitic activity. Further research to clarify the mechanisms that lead to antiparasitic activity is envisaged.

### 3. Materials and Methods

#### 3.1. Chemistry

The chemistry experimental part, with full description of procedures and characterization data for all compounds, is presented in the Supplementary Materials.

#### 3.2. Biological Evaluation

##### 3.2.1. Cell and Parasite Culture

All tissue culture media were purchased from Gibco-BRL, and biochemical agents were purchased from Sigma-Aldrich. Human foreskin fibroblasts (HFF) were purchased from ATCC, maintained in DMEM (Dulbecco's Modified Eagle's Medium) supplemented with 10% fetal calf serum (FCS, Gibco-BRL, Waltham, MA, USA) and antibiotics as previously described [60]. Transgenic *T. gondii*  $\beta$ -gal (expressing the  $\beta$ -galactosidase gene from *Escherichia coli*) were kindly provided by Prof. David Sibley (Washington University, St. Louis, MO, USA) and were maintained, isolated, and prepared for new infections as shown before [60,127].

##### 3.2.2. In Vitro Assessment against *T. gondii* Tachyzoites and Human Foreskin Fibroblasts

The screening cascade for the compounds was described in former studies [111]. All compounds were prepared as 1 mM stock solutions from powder, in dimethyl sulfoxide (DMSO, Sigma, St. Louis, MO, USA). For in vitro activity and cytotoxicity assays, HFF were seeded at  $5 \times 10^3$ /well and allowed to grow to confluence in phenol-red free culture medium at 37 °C and 5% CO<sub>2</sub>. *T. gondii* tachyzoites were released from host cells, and HFF monolayers were infected with freshly isolated parasites ( $1 \times 10^3$ /well), and compounds were added concomitantly with infection.

In the primary screening, HFF monolayers infected with *T. gondii*  $\beta$ -gal were treated with 0.1 and 1  $\mu$ M of each compound, or the corresponding concentration of DMSO (0.01 or 0.1%, respectively) as controls and were incubated for 72 h at 37 °C/5% CO<sub>2</sub> as previously described [128].

For the dose-response study (IC<sub>50</sub> values), measurements for *T. gondii*  $\beta$ -gal were performed. The selected compounds were added concomitantly with infection in 8 serial concentrations 0.007, 0.01, 0.03, 0.06, 0.12, 0.25, 0.5, and 1  $\mu$ M.

To measure the activity of the tested compound on *T. gondii*  $\beta$ -gal parasites, after a period of 72 h of culture at 37 °C/5% CO<sub>2</sub>, the culture medium was aspirated, and cells were permeabilized by adding 90  $\mu$ L PBS (phosphate buffered saline) with 0.05% Triton X-100. Next, 10  $\mu$ L of 5 mM chlorophenolred- $\beta$ -D-galactopyranoside (CPRG; Roche Diagnostics, Rotkreuz, Switzerland, substrate for the  $\beta$ -galactosidase) in PBS were added. Release of chlorophenol red was measured at 570 nm using an EnSpire® multimode plate reader (PerkinElmer, Inc., Waltham, MA, USA). A 100% proliferation of *T. gondii*  $\beta$ -gal was

assigned to control parasites treated only with DMSO. For the primary screening at 0.1 and 1  $\mu\text{M}$ , the activity was measured as the release of chlorophenol red over time and was calculated as percentage from the respective DMSO treated control, which represented 100% of *T. gondii*  $\beta$ -gal growth.

For the  $\text{IC}_{50}$  assays, the activity measured as the release of chlorophenol red over time was proportional to the number of live parasites down to 50 per well as determined in pilot assays.  $\text{IC}_{50}$  values were calculated after the logit-log-transformation of relative growth and subsequent regression analysis. All calculations were performed using the corresponding software tool contained in the Excel software package (Microsoft, Redmond, WA, USA).

Cytotoxicity assays using uninfected confluent HFF host cells were performed by the alamarBlue assay as previously reported [129]. Confluent HFF monolayers in 96 well-plates were exposed to 0.1, 1, and 2.5  $\mu\text{M}$  of each compound. Non-treated HFF as well as DMSO controls (0.01%, 0.1%, and 0.25%) were included. After 72 h of incubation at 37  $^{\circ}\text{C}$ /5%  $\text{CO}_2$ , the medium was removed, and the plates were washed once with PBS. Resazurin suspended in PBS to a final concentration of 0.01 g/L was added to each well (200  $\mu\text{L}$ /well). Fluorescence was measured at excitation wavelength 530 nm and emission wavelength 590 nm using an EnSpire<sup>®</sup> multimode plate reader (PerkinElmer, Inc, Waltham, MA, USA). The cytotoxicity values were calculated as percentage of the respective DMSO control, which represented 100% of HFF viability.

#### 4. Conclusions

This study was focused on the synthesis and antiparasitic activity assessment of nucleobase-tethered trithiolato-bridged dinuclear ruthenium(II)-arene compounds, aiming at exploiting the parasite auxotrophies and metabolic peculiarities for nucleic bases. Various synthetic strategies and structural modifications were considered, affording 23 new diruthenium conjugates. The CuAAC reactions proved to be a convenient method for the functionalization of trithiolato diruthenium compounds with various substrates including nucleobase derivatives. The organometallic fragment was used both as alkyne and azide group bearing partner and allowed the isolation of 19 new click conjugates. The conjugate synthesis based on CuAAC reactions can be used to develop other thiolato-bridged ruthenium(II)-arene hybrids in a convenient manner and to construct larger libraries of compounds.

The antiparasitic activity and the toxicity on the host cells were influenced not only by the nature of the molecule appended to the diruthenium scaffold but also by the linker between the two moieties. Even though some of the compounds presented in this study exhibit good antitoxoplasma activity and low HFF toxicity, when considering the overall results, targeting *T. gondii* metabolic pathways using nucleobase conjugates of trithiolato diruthenium derivatives does not appear to be a promising approach as the hybrid molecules presenting nucleic base units did not necessarily performed better compared to conjugates presenting other types of substituents. However, further evaluations of the conjugates against other nucleobase auxotrophic parasites, such as *Leishmania donovani* and *Plasmodium* should be performed to conclusively appraise the proposed strategy.

Ester **14**, conjugated to 9-(2-oxethyl)adenine, and click product **36**, bearing a 2-(4-(hydroxymethyl)-1*H*-1,2,3-triazol-1-yl)methyl substituent, exhibited interesting  $\text{IC}_{50}$  values on *T. gondii*  $\beta$ -gal of 0.059 and 0.111  $\mu\text{M}$ , respectively, with only medium toxicity to HFF at 2.5  $\mu\text{M}$ . These two hybrid molecules deserve further investigations.

**Supplementary Materials:** The following supporting information can be downloaded at: <https://www.mdpi.com/article/10.3390/molecules27238173/s1>, Synthetical procedures; Synthesis of the trithiolato-bridged dinuclear ruthenium(II)-arene intermediates **5–7** and **9, 10**; Synthesis of the conjugates **11–13** (family 1); Synthesis of the compounds **14** (family 2); Synthesis of the compounds **15–26** (family 3); Synthesis of the compounds **27–33** (family 4); Synthesis of the compounds **34–39** (family 5). Figure S1.  $^1\text{H}$  NMR spectra of **4** and **24** recorded in  $\text{DMSO}-d_6$  at 25  $^{\circ}\text{C}$ ; (A) recorded 5 min after sample preparation, and (B) sample after >100 days storage at 0–5  $^{\circ}\text{C}$  in the dark. Figure S2.  $^1\text{H}$  NMR spectra of **28, 33**, and **39** recorded in  $\text{DMSO}-d_6$  at 25  $^{\circ}\text{C}$ ; (A) recorded 5 min after sample

preparation, and (B) sample after > 100 days storage at 0–5 °C in the dark; Figure S3. Study of H-bond interactions with complementary nucleobases by <sup>1</sup>H NMR at r.t. for cytosine conjugate **25** and guanine; Figure S4. Study of H-bond interactions with complementary nucleobases by <sup>1</sup>H NMR for uracil conjugate **23** and adenine; Figure S5. Study of H-bond interactions with complementary nucleobases by <sup>1</sup>H NMR at r.t. for thymine conjugate **24** and adenine; Figure S6. Study of H-bond interactions with complementary nucleobases by <sup>1</sup>H NMR for adenine conjugate **26** and uracil; Figure S7. Study of H-bond interactions with complementary nucleobases by <sup>1</sup>H NMR for adenine conjugate **26** and thymine; References [93,96,101,111,112,115,117,118,128,130–133] are cited in Supplementary Materials.

**Author Contributions:** Conceptualization, A.H., J.F. and E.P.; Methodology, O.D., G.B., A.H., J.F. and E.P.; Software, M.M., Y.A., O.D., N.A., G.B. and E.P.; Validation, O.D., G.B., A.H., J.F. and E.P.; Formal Analysis, M.M., Y.A., O.D., N.A., G.B. and E.P.; Investigation, M.M., Y.A., O.D., N.A., G.B. and E.P.; Resources, A.H. and J.F.; Data Curation, O.D., G.B., N.A., J.F., A.H. and E.P.; Writing—Original Draft Preparation, O.D., G.B., N.A. and E.P.; Writing—Review & Editing, O.D., G.B., N.A., A.H., J.F. and E.P.; Supervision, G.B., A.H., J.F. and E.P.; Project Administration, A.H. and J.F.; Funding Acquisition, A.H. and J.F. All authors have read and agreed to the published version of the manuscript.

**Funding:** This work was financially supported by the Swiss Science National Foundation (SNF, Sinergia project CRSII5-173718 and project no. 310030\_184662).

**Institutional Review Board Statement:** Not applicable.

**Informed Consent Statement:** Not applicable.

**Data Availability Statement:** The data are included in the article and Supplementary Materials.

**Conflicts of Interest:** The authors declare no conflict of interest.

## References

1. Torgerson, P.R.; Devleeschauwer, B.; Praet, N.; Speybroeck, N.; Willingham, A.L.; Kasuga, F.; Rokni, M.B.; Zhou, X.N.; Fevre, E.M.; Sripa, B.; et al. World Health Organization estimates of the global and regional disease burden of 11 foodborne parasitic diseases, 2010: A data synthesis. *PLoS Med.* **2015**, *12*, e1001920. [[CrossRef](#)] [[PubMed](#)]
2. Meireles, L.R.; Ekman, C.C.; Andrade Jr, H.F.; Luna, E.J. Human toxoplasmosis outbreaks and the agent infecting form. Findings from a systematic review. *Rev. Inst. Med. Trop. Sao Paulo* **2015**, *57*, 369–376. [[CrossRef](#)]
3. Neville, A.J.; Zach, S.J.; Wang, X.; Larson, J.J.; Judge, A.K.; Davis, L.A.; Vennerstrom, J.L.; Davis, P.H. Clinically available medicines demonstrating anti-Toxoplasma activity. *Antimicrob. Agents Chemother.* **2015**, *59*, 7161–7169. [[CrossRef](#)] [[PubMed](#)]
4. Vargas-Villavicencio, J.A.; Besne-Merida, A.; Correa, D. Vertical transmission and fetal damage in animal models of congenital toxoplasmosis: A systematic review. *Vet. Parasitol.* **2016**, *223*, 195–204. [[CrossRef](#)] [[PubMed](#)]
5. Alday, P.H.; Doggett, J.S. Drugs in development for toxoplasmosis: Advances, challenges, and current status. *Drug Des. Dev. Ther.* **2017**, *11*, 273–293. [[CrossRef](#)]
6. Konstantinovic, N.; Guegan, H.; Stajner, T.; Belaz, S.; Robert-Gangneux, F. Treatment of toxoplasmosis: Current options and future perspectives. *Food Waterborne Parasitol.* **2019**, *15*, e00036. [[CrossRef](#)]
7. Sibley, L.D. *Toxoplasma gondii*: Perfecting an intracellular life style. *Traffic* **2003**, *4*, 581–586. [[CrossRef](#)]
8. Coppens, I. Exploitation of auxotrophies and metabolic defects in Toxoplasma as therapeutic approaches. *Int. J. Parasitol.* **2014**, *44*, 109–120. [[CrossRef](#)]
9. Krug, E.C.; Marr, J.J.; Berens, R.L. Purine metabolism in *Toxoplasma gondii*. *J. Biol. Chem.* **1989**, *264*, 10601–10607. [[CrossRef](#)]
10. Chaudhary, K.; Darling, J.A.; Fohl, L.M.; Sullivan, W.J., Jr.; Donald, R.G.; Pfefferkorn, E.R.; Ullman, B.; Roos, D.S. Purine salvage pathways in the apicomplexan parasite *Toxoplasma gondii*. *J. Biol. Chem.* **2004**, *279*, 31221–31227. [[CrossRef](#)]
11. Perrotto, J.; Keister, D.B.; Gelderman, A.H. Incorporation of precursors into Toxoplasma DNA. *J. Protozool.* **1971**, *18*, 470–473. [[CrossRef](#)]
12. Fox, B.A.; Bzik, D.J. Biochemistry and metabolism of *Toxoplasma gondii*: Purine and pyrimidine acquisition in *Toxoplasma gondii* and other Apicomplexa. In *Toxoplasma gondii. The Model Apicomplexan—Perspectives and Methods*, 3rd ed.; Weiss, L.M., Kim, K., Eds.; Academic Press: Cambridge, MA, USA, 2020; pp. 397–449.
13. Fox, B.A.; Bzik, D.J. De novo pyrimidine biosynthesis is required for virulence of *Toxoplasma gondii*. *Nature* **2002**, *415*, 926–929. [[CrossRef](#)] [[PubMed](#)]
14. Fox, B.A.; Bzik, D.J. Avirulent uracil auxotrophs based on disruption of orotidine-5'-monophosphate decarboxylase elicit protective immunity to *Toxoplasma gondii*. *Infect. Immun.* **2010**, *78*, 3744–3752. [[CrossRef](#)] [[PubMed](#)]
15. Schwartzman, J.D.; Pfefferkorn, E.R. Pyrimidine synthesis by intracellular *Toxoplasma gondii*. *J. Parasitol.* **1981**, *67*, 150–158. [[CrossRef](#)] [[PubMed](#)]
16. Iltzsch, M.H. Pyrimidine salvage pathways in *Toxoplasma gondii*. *J. Eukaryot Microbiol.* **1993**, *40*, 24–28. [[CrossRef](#)]

17. Hajj, R.E.; Tawk, L.; Itani, S.; Hamie, M.; Ezzeddine, J.; El Sabban, M.; El Hajj, H. Toxoplasmosis: Current and emerging parasite druggable targets. *Microorganisms* **2021**, *9*, 531. [\[CrossRef\]](#)
18. Wu, R.Z.; Zhou, H.Y.; Song, J.F.; Xia, Q.H.; Hu, W.; Mou, X.D.; Li, X. Chemotherapeutics for *Toxoplasma gondii*: Molecular biotargets, binding modes, and structure-activity relationship investigations. *J. Med. Chem.* **2021**, *64*, 17627–17655. [\[CrossRef\]](#)
19. Cajazeiro, D.C.; Toledo, P.P.M.; de Sousa, N.F.; Scotti, M.T.; Reimao, J.Q. Drug repurposing based on protozoan proteome: In vitro evaluation of in silico screened compounds against *Toxoplasma gondii*. *Pharmaceutics* **2022**, *14*, 1634. [\[CrossRef\]](#)
20. Silva, M.D.; Teixeira, C.; Gomes, P.; Borges, M. Promising drug targets and compounds with anti-*Toxoplasma gondii* activity. *Microorganisms* **2021**, *9*, 1960. [\[CrossRef\]](#)
21. Hopper, A.T.; Brockman, A.; Wise, A.; Gould, J.; Barks, J.; Radke, J.B.; Sibley, L.D.; Zou, Y.; Thomas, S. Discovery of Selective *Toxoplasma gondii* Dihydrofolate Reductase Inhibitors for the Treatment of Toxoplasmosis. *J. Med. Chem.* **2019**, *62*, 1562–1576. [\[CrossRef\]](#)
22. Jiang, L.; Liu, B.; Hou, S.; Su, T.; Fan, Q.; Alyafeai, E.; Tang, Y.; Wu, M.; Liu, X.; Li, J.; et al. Discovery and evaluation of chalcone derivatives as novel potential anti-*Toxoplasma gondii* agents. *Eur. J. Med. Chem.* **2022**, *234*, 114244. [\[CrossRef\]](#)
23. Sadeghi, M.; Sarvi, S.; Emami, S.; Khalilian, A.; Hosseini, S.A.; Montazeri, M.; Shahdin, S.; Nayeri, T.; Daryani, A. Evaluation of anti-parasitic activities of new quinolones containing nitrofuranyl moiety against *Toxoplasma gondii*. *Exp. Parasitol.* **2022**, *240*, 108344. [\[CrossRef\]](#) [\[PubMed\]](#)
24. Weglinska, L.; Bekier, A.; Trotsko, N.; Kapron, B.; Plech, T.; Dzitko, K.; Paneth, A. Inhibition of *Toxoplasma gondii* by 1,2,4-triazole-based compounds: Marked improvement in selectivity relative to the standard therapy pyrimethamine and sulfadiazine. *J. Enzyme Inhib. Med. Chem.* **2022**, *37*, 2621–2634. [\[CrossRef\]](#)
25. Bekier, A.; Gatkowska, J.; Chyb, M.; Sokolowska, J.; Chwatko, G.; Glowacki, R.; Paneth, A.; Dzitko, K. 4-Arylthiosemicarbazide derivatives—Pharmacokinetics, toxicity and anti-*Toxoplasma gondii* activity in vivo. *Eur. J. Med. Chem.* **2022**, *244*, 114812. [\[CrossRef\]](#) [\[PubMed\]](#)
26. Molina, D.A.; Ramos, G.A.; Zamora-Velez, A.; Gallego-Lopez, G.M.; Rocha-Roa, C.; Gomez-Marin, J.E.; Cortes, E. In vitro evaluation of new 4-thiazolidinones on invasion and growth of *Toxoplasma gondii*. *Int. J. Parasitol. Drugs Drug Resist.* **2021**, *16*, 129–139. [\[CrossRef\]](#) [\[PubMed\]](#)
27. Araujo-Silva, C.A.; De Souza, W.; Martins-Duarte, E.S.; Vommaro, R.C. HDAC inhibitors Tubastatin A and SAHA affect parasite cell division and are potential anti-*Toxoplasma gondii* chemotherapeutics. *Int. J. Parasitol. Drugs Drug Resist.* **2021**, *15*, 25–35. [\[CrossRef\]](#)
28. Imhof, D.; Anghel, N.; Winzer, P.; Balmer, V.; Ramseier, J.; Hanggeli, K.; Choi, R.; Hulverson, M.A.; Whitman, G.R.; Arnold, S.L.M.; et al. In vitro activity, safety and in vivo efficacy of the novel bumped kinase inhibitor BKI-1748 in non-pregnant and pregnant mice experimentally infected with *Neospora caninum* tachyzoites and *Toxoplasma gondii* oocysts. *Int. J. Parasitol. Drugs Drug Resist.* **2021**, *16*, 90–101. [\[CrossRef\]](#)
29. Doggett, J.S.; Schultz, T.; Miller, A.J.; Bruzual, I.; Pou, S.; Winter, R.; Dodean, R.; Zakharov, L.N.; Nilsen, A.; Riscoe, M.K.; et al. Orally bioavailable endochin-like quinolone carbonate ester prodrug reduces *Toxoplasma gondii* brain cysts. *Antimicrob. Agents Chemother.* **2020**, *64*, e00535-20. [\[CrossRef\]](#)
30. Muller, J.; Boubaker, G.; Imhof, D.; Hanggeli, K.; Haudenschild, N.; Uldry, A.C.; Braga-Lagache, S.; Heller, M.; Ortega-Mora, L.M.; Hemphill, A. Differential affinity chromatography coupled to mass spectrometry: A suitable tool to identify common binding proteins of a broad-range antimicrobial peptide derived from leucinoastatin. *Biomedicines* **2022**, *10*, 2675. [\[CrossRef\]](#)
31. Martynowicz, J.; Doggett, J.S.; Sullivan, W.J., Jr. Efficacy of Guanabenz combination therapy against chronic toxoplasmosis across multiple mouse strains. *Antimicrob. Agents Chemother.* **2020**, *64*, e00539-20. [\[CrossRef\]](#)
32. Hammarton, T.C.; Mottram, J.C.; Doerig, C. The cell cycle of parasitic protozoa: Potential for chemotherapeutic exploitation. *Prog. Cell. Cycle Res.* **2003**, *5*, 91–101. [\[PubMed\]](#)
33. Mukherjee, S.; Mukherjee, N.; Gayen, P.; Roy, P.; Babu, S.P. Metabolic inhibitors as antiparasitic drugs: Pharmacological, biochemical and molecular perspectives *Curr. Drug. Metab.* **2016**, *17*, 937–970. [\[CrossRef\]](#) [\[PubMed\]](#)
34. de Koning, H.P.; Bridges, D.J.; Burchmore, R.J. Purine and pyrimidine transport in pathogenic protozoa: From biology to therapy. *FEMS Microbiol. Rev.* **2005**, *29*, 987–1020. [\[CrossRef\]](#) [\[PubMed\]](#)
35. el Kouni, M.H. Potential chemotherapeutic targets in the purine metabolism of parasites. *Pharmacol. Ther.* **2003**, *99*, 283–309. [\[CrossRef\]](#) [\[PubMed\]](#)
36. el Kouni, M.H. Adenosine metabolism in *Toxoplasma gondii*: Potential targets for chemotherapy. *Curr. Pharm. Des.* **2007**, *13*, 581–597. [\[CrossRef\]](#)
37. Wang, Y.; Karnataki, A.; Parsons, M.; Weiss, L.M.; Orlofsky, A. 3-Methyladenine blocks *Toxoplasma gondii* division prior to centrosome replication. *Mol. Biochem. Parasitol.* **2010**, *173*, 142–153. [\[CrossRef\]](#)
38. Kim, Y.A.; Rawal, R.K.; Yoo, J.; Sharon, A.; Jha, A.K.; Chu, C.K.; Rais, R.H.; Al Safarjalani, O.N.; Naguib, F.N.; El Kouni, M.H. Structure-activity relationships of carbocyclic 6-benzylthioinosine analogues as subversive substrates of *Toxoplasma gondii* adenosine kinase. *Bioorg. Med. Chem.* **2010**, *18*, 3403–3412. [\[CrossRef\]](#)
39. Kim, Y.A.; Sharon, A.; Chu, C.K.; Rais, R.H.; Al Safarjalani, O.N.; Naguib, F.N.; el Kouni, M.H. Synthesis, biological evaluation and molecular modeling studies of N6-benzyladenosine analogues as potential anti-toxoplasma agents. *Biochem. Pharmacol.* **2007**, *73*, 1558–1572. [\[CrossRef\]](#)

40. Gherardi, A.; Sarciron, M.E. Molecules targeting the purine salvage pathway in apicomplexan parasites. *Trends Parasitol.* **2007**, *23*, 384–389. [\[CrossRef\]](#)
41. Sullivan, W.J., Jr.; Dixon, S.E.; Li, C.; Striepen, B.; Queener, S.F. IMP dehydrogenase from the protozoan parasite *Toxoplasma gondii*. *Antimicrob. Agents Chemother.* **2005**, *49*, 2172–2179. [\[CrossRef\]](#)
42. Al Safarjalani, O.N.; Naguib, F.N.; El Kouni, M.H. Uptake of nitrobenzylthioinosine and purine beta-L-nucleosides by intracellular *Toxoplasma gondii*. *Antimicrob. Agents Chemother.* **2003**, *47*, 3247–3251. [\[CrossRef\]](#) [\[PubMed\]](#)
43. Azzouz, S.; Lawton, P. In vitro effects of purine and pyrimidine analogues on *Leishmania donovani* and *Leishmania infantum* promastigotes and intracellular amastigotes. *Acta Parasitol.* **2017**, *62*, 582–588. [\[CrossRef\]](#)
44. Al Safarjalani, O.N.; Rais, R.H.; Kim, Y.A.; Chu, C.K.; Naguib, F.N.; El Kouni, M.H. Carbocyclic 6-benzylthioinosine analogues as subversive substrates of *Toxoplasma gondii* adenosine kinase: Biological activities and selective toxicities. *Biochem. Pharmacol.* **2010**, *80*, 955–963. [\[CrossRef\]](#)
45. Donaldson, T.M.; Cassera, M.B.; Ho, M.C.; Zhan, C.; Merino, E.F.; Evans, G.B.; Tyler, P.C.; Almo, S.C.; Schramm, V.L.; Kim, K. Inhibition and structure of *Toxoplasma gondii* purine nucleoside phosphorylase. *Eukaryot Cell* **2014**, *13*, 572–579. [\[CrossRef\]](#)
46. Anthony, E.J.; Bolitho, E.M.; Bridgewater, H.E.; Carter, O.W.L.; Donnelly, J.M.; Imberti, C.; Lant, E.C.; Lermite, F.; Needham, R.J.; Palau, M.; et al. Metallodrugs are unique: Opportunities and challenges of discovery and development *Chem. Sci.* **2020**, *11*, 12888–12917. [\[CrossRef\]](#) [\[PubMed\]](#)
47. Loginova, N.V.; Harbatsevich, H.I.; Osipovich, N.P.; Ksendzova, G.A.; Koval'chuk, T.V.; Polozov, G.I. Metal complexes as promising agents for biomedical applications. *Curr. Med. Chem.* **2020**, *27*, 5213–5249. [\[CrossRef\]](#) [\[PubMed\]](#)
48. Ong, Y.C.; Gasser, G. Organometallic compounds in drug discovery: Past, present and future. *Drug Discov. Today Technol.* **2020**, *37*, 117–124. [\[CrossRef\]](#)
49. Konkankit, C.C.; Marker, S.C.; Knopf, K.M.; Wilson, J.J. Anticancer activity of complexes of the third row transition metals, rhenium, osmium, and iridium. *Dalton Trans.* **2018**, *47*, 9934–9974. [\[CrossRef\]](#)
50. Simpson, P.V.; Desai, N.M.; Casari, I.; Massi, M.; Falasca, M. Metal-based antitumor compounds: Beyond cisplatin. *Future Med. Chem.* **2019**, *11*, 119–135. [\[CrossRef\]](#)
51. Gasser, G.; Ott, I.; Metzler-Nolte, N. Organometallic anticancer compounds. *J. Med. Chem.* **2011**, *54*, 3–25. [\[CrossRef\]](#)
52. Deng, Y.; Wu, T.; Zhai, S.Q.; Li, C.H. Recent progress on anti-Toxoplasma drugs discovery: Design, synthesis and screening. *Eur. J. Med. Chem.* **2019**, *183*, 111711. [\[CrossRef\]](#) [\[PubMed\]](#)
53. Mbaba, M.; Golding, T.M.; Smith, G.S. Recent advances in the biological investigation of organometallic platinum-group metal (Ir, Ru, Rh, Os, Pd, Pt) complexes as antimalarial agents. *Molecules* **2020**, *25*, 5276. [\[CrossRef\]](#)
54. Gambino, D.; Otero, L. Design of prospective antiparasitic metal-based compounds including selected organometallic cores. *Inorg. Chim. Acta* **2018**, *472*, 58–75. [\[CrossRef\]](#)
55. Navarro, M.; Justo, R.M.S.; Delgado, G.Y.S.; Visbal, G. Metallodrugs for the treatment of Trypanosomatid diseases: Recent advances and new insights. *Curr. Pharm. Des.* **2021**, *27*, 1763–1789. [\[CrossRef\]](#) [\[PubMed\]](#)
56. Brown, R.W.; Hyland, C.J.T. Medicinal organometallic chemistry—An emerging strategy for the treatment of neglected tropical diseases *Med. Chem. Commun.* **2015**, *6*, 1230–1243. [\[CrossRef\]](#)
57. Ong, Y.C.; Roy, S.; Andrews, P.C.; Gasser, G. Metal compounds against neglected tropical diseases. *Chem. Rev.* **2019**, *119*, 730–796. [\[CrossRef\]](#) [\[PubMed\]](#)
58. Coverdale, J.P.C.; Laroia-McCarron, T.; Romero-Canelón, I. Designing ruthenium anticancer drugs: What have we learnt from the key drug candidates? *Inorganics* **2019**, *7*, 31. [\[CrossRef\]](#)
59. Lee, S.Y.; Kim, C.Y.; Nam, T.G. Ruthenium complexes as anticancer agents: A brief history and perspectives. *Drug Des. Dev. Ther.* **2020**, *14*, 5375–5392. [\[CrossRef\]](#) [\[PubMed\]](#)
60. Barna, F.; Debache, K.; Vock, C.A.; Kuster, T.; Hemphill, A. In vitro effects of novel ruthenium complexes in *Neospora caninum* and *Toxoplasma gondii* tachyzoites. *Antimicrob. Agents Chemother.* **2013**, *57*, 5747–5754. [\[CrossRef\]](#) [\[PubMed\]](#)
61. Gambino, D.; Otero, L. Perspectives on what ruthenium-based compounds could offer in the development of potential antiparasitic drugs. *Inorg. Chim. Acta* **2012**, *393*, 103–114. [\[CrossRef\]](#)
62. Adams, M.; Li, Y.; Khot, H.; De Kock, C.; Smith, P.J.; Land, K.; Chibale, K.; Smith, G.S. The synthesis and antiparasitic activity of aryl- and ferrocenyl-derived thiosemicarbazone ruthenium(II)-arene complexes. *Dalton Trans.* **2013**, *42*, 4677–4685. [\[CrossRef\]](#) [\[PubMed\]](#)
63. Fernandez, M.; Arce, E.R.; Sarniguet, C.; Morais, T.S.; Tomaz, A.I.; Azar, C.O.; Figueroa, R.; Diego Maya, J.; Medeiros, A.; Comini, M.; et al. Novel ruthenium(II) cyclopentadienyl thiosemicarbazone compounds with antiproliferative activity on pathogenic trypanosomatid parasites. *J. Inorg. Biochem.* **2015**, *153*, 306–314. [\[CrossRef\]](#) [\[PubMed\]](#)
64. Stringer, T.; Quintero, M.A.S.; Wiesner, L.; Smith, G.S.; Nordlander, E. Evaluation of PTA-derived ruthenium(II) and iridium(III) quinoline complexes against chloroquine-sensitive and resistant strains of the *Plasmodium falciparum* malaria parasite. *J. Inorg. Biochem.* **2019**, *191*, 164–173. [\[CrossRef\]](#)
65. Fandzloch, M.; Jedrzejewski, T.; Dobrzanska, L.; Esteban-Parra, G.M.; Wisniewska, J.; Paneth, A.; Paneth, P.; Sitkowski, J. New organometallic ruthenium(II) complexes with purine analogs—A wide perspective on their biological application. *Dalton Trans.* **2021**, *50*, 5557–5573. [\[CrossRef\]](#)
66. Wang, X.; Guo, Z. Targeting and delivery of platinum-based anticancer drugs. *Chem. Soc. Rev.* **2013**, *42*, 202–224. [\[CrossRef\]](#)

67. Kenny, R.G.; Marmion, C.J. Toward multi-targeted platinum and ruthenium drugs—A new paradigm in cancer drug treatment regimens? *Chem. Rev.* **2019**, *119*, 1058–1137. [\[CrossRef\]](#) [\[PubMed\]](#)
68. Zhao, Y.; Kang, Y.; Xu, F.; Zheng, W.; Luo, Q.; Zhang, Y.; Jia, F.; Wang, F. Pharmacophore conjugation strategy for multi-targeting metal-based anticancer complexes. In *Advances in Inorganic Chemistry*; Sadler, P.J., van Eldik, R., Eds.; Academic Press: Cambridge, MA, USA, 2020; Volume 75, pp. 257–285.
69. Kowalski, K. Organometallic nucleosides—Synthesis, transformations, and applications *Coord. Chem. Rev.* **2021**, *432*, 213705. [\[CrossRef\]](#)
70. Kowalski, K. Ferrocenyl-nucleobase complexes: Synthesis, chemistry and applications. *Coord. Chem. Rev.* **2016**, *317*, 132–156. [\[CrossRef\]](#)
71. Singh, A.; Lumb, I.; Mehra, V.; Kumar, V. Ferrocene-appended pharmacophores: An exciting approach for modulating the biological potential of organic scaffolds. *Dalton Trans.* **2019**, *48*, 2840–2860. [\[CrossRef\]](#)
72. Daniluk, M.; Buchowicz, W.; Koszytkowska-Stawińska, M.; Jarzabek, K.; Jarzemska, K.N.; Kamiński, R.; Piszcz, M.; Laudy, A.E.; Tyski, S. Ferrocene amino acid ester uracil conjugates: Synthesis, structure, electrochemistry and antimicrobial evaluation. *ChemistrySelect* **2019**, *4*, 11130–11135. [\[CrossRef\]](#)
73. James, P.; Neudorfl, J.; Eissmann, M.; Jesse, P.; Prokop, A.; Schmalz, H.G. Enantioselective synthesis of ferrocenyl nucleoside analogues with apoptosis-inducing activity. *Org. Lett.* **2006**, *8*, 2763–2766. [\[CrossRef\]](#) [\[PubMed\]](#)
74. Florindo, P.R.; Pereira, D.M.; Borralho, P.M.; Piedade, M.F.M.; Conceição Oliveira, M.; Dias, A.M.; Rodrigues, C.M.P.; Fernandes, A.C. Organoruthenium(II) nucleoside conjugates as colon cytotoxic agents. *New J. Chem.* **2019**, *43*, 1195–1205. [\[CrossRef\]](#)
75. Leitao, M.I.P.S.; Herrera, F.; Petronilho, A. N-Heterocyclic Carbenes Derived from Guanosine: Synthesis and Evidences of Their Antiproliferative Activity. *ACS Omega* **2018**, *3*, 15653–15656. [\[CrossRef\]](#) [\[PubMed\]](#)
76. Collado, A.; Gómez-Gallego, M.; Sierra, M.A. Nucleobases having M–C bonds: An emerging bio-organometallic field. *Eur. J. Org. Chem.* **2018**, *2018*, 1617–1623. [\[CrossRef\]](#)
77. Kaczmarek, R.; Korczynski, D.; Krolewska-Golinska, K.; Wheeler, K.A.; Chavez, F.A.; Mikus, A.; Dembinski, R. Organometallic nucleosides: Synthesis and biological evaluation of substituted dicobalt hexacarbonyl 2'-deoxy-5-oxopropynyluridines. *ChemistryOpen* **2018**, *7*, 237–247. [\[CrossRef\]](#) [\[PubMed\]](#)
78. Nguyen, H.V.; Sallustrau, A.; Balzarini, J.; Bedford, M.R.; Eden, J.C.; Georgousi, N.; Hodges, N.J.; Kedge, J.; Mehellou, Y.; Tselepis, C.; et al. Organometallic nucleoside analogues with ferrocenyl linker groups: Synthesis and cancer cell line studies. *J. Med. Chem.* **2014**, *57*, 5817–5822. [\[CrossRef\]](#) [\[PubMed\]](#)
79. Ismail, M.K.; Khan, Z.; Rana, M.; Horswell, S.L.; Male, L.; Nguyen, H.V.; Perotti, A.; Romero-Canelon, I.; Wilkinson, E.A.; Hodges, N.J.; et al. Effect of regiochemistry and methylation on the anticancer activity of a ferrocene-containing organometallic nucleoside analogue. *ChemBioChem* **2020**, *21*, 2487–2494. [\[CrossRef\]](#)
80. Skiba, J.; Kowalski, K.; Prochnicka, A.; Ott, I.; Solecka, J.; Rajnisz, A.; Therrien, B. Metallocene-uracil conjugates: Synthesis and biological evaluation of novel mono-, di- and tri-nuclear systems. *J. Organomet. Chem.* **2015**, *782*, 52–61. [\[CrossRef\]](#)
81. Singh, A.; Biot, C.; Viljoen, A.; Dupont, C.; Kremer, L.; Kumar, K.; Kumar, V. 1H-1,2,3-triazole-tethered uracil-ferrocene and uracil-ferrocenylchalcone conjugates: Synthesis and antitubercular evaluation. *Chem. Biol. Drug Des.* **2017**, *89*, 856–861. [\[CrossRef\]](#) [\[PubMed\]](#)
82. Rep, V.; Piskor, M.; Simek, H.; Misetic, P.; Grbic, P.; Padovan, J.; Gabelica Markovic, V.; Jadresko, D.; Pavelic, K.; Kraljevic Pavelic, S.; et al. Purine and purine isostere derivatives of ferrocene: An evaluation of ADME, antitumor and electrochemical properties. *Molecules* **2020**, *25*, 1570. [\[CrossRef\]](#)
83. Djaković, S.; Glavaš-Obrovac, L.; Lapić, J.; Marčić, S.; Kirchofer, J.; Knežević, M.; Jukić, M.; Raić-Malić, S. Synthesis and biological evaluations of mono- and bis-ferrocene uracil derivatives. *Appl. Organomet. Chem.* **2020**, *35*, e6052. [\[CrossRef\]](#)
84. Kowalski, K.; Szczupak, L.; Saloman, S.; Steverding, D.; Jablonski, A.; Vrcek, V.; Hildebrandt, A.; Lang, H.; Rybarczyk-Pirek, A. Cymantrene, cyrhetrene and ferrocene nucleobase conjugates: Synthesis, structure, computational study, electrochemistry and antitrypanosomal activity. *ChemPlusChem* **2017**, *82*, 303–314. [\[CrossRef\]](#) [\[PubMed\]](#)
85. Liu, K.-G.; Cai, X.-Q.; Li, X.-C.; Qin, D.-A.; Hu, M.-L. Arene-ruthenium(II) complexes containing 5-fluorouracil-1-methyl isonicotinate: Synthesis and characterization of their anticancer activity. *Inorg. Chim. Acta* **2012**, *388*, 78–83. [\[CrossRef\]](#)
86. Li, Z.J.; Hou, Y.; Qin, D.A.; Jin, Z.M.; Hu, M.L. Two half-sandwiched ruthenium (II) compounds containing 5-fluorouracil derivatives: Synthesis and study of DNA intercalation. *PLoS ONE* **2015**, *10*, e0120211. [\[CrossRef\]](#) [\[PubMed\]](#)
87. Florindo, P.R.; Pereira, D.M.; Borralho, P.M.; Costa, P.J.M.; Rodrigues, C.M.P.; Piedade, M.F.M.; Fernandes, A.C. New [(η<sup>5</sup>-C<sub>5</sub>H<sub>5</sub>)Ru(N–N)(PPh<sub>3</sub>)](PF<sub>6</sub>) compounds: Colon anticancer activity and GLUT-mediated cellular uptake of carbohydrate-appended complexes. *Dalton Trans.* **2016**, *45*, 11926–11930. [\[CrossRef\]](#)
88. Furrer, J.; Süss-Fink, G. Thiolato-bridged dinuclear arene ruthenium complexes and their potential as anticancer drugs. *Coord. Chem. Rev.* **2016**, *309*, 36–50. [\[CrossRef\]](#)
89. Basto, A.P.; Anghel, N.; Rubbiani, R.; Muller, J.; Stibal, D.; Giannini, F.; Süss-Fink, G.; Balmer, V.; Gasser, G.; Furrer, J.; et al. Targeting of the mitochondrion by dinuclear thiolato-bridged arene ruthenium complexes in cancer cells and in the apicomplexan parasite *Neospora caninum*. *Metallomics* **2019**, *11*, 462–474. [\[CrossRef\]](#)
90. Basto, A.P.; Muller, J.; Rubbiani, R.; Stibal, D.; Giannini, F.; Süss-Fink, G.; Balmer, V.; Hemphill, A.; Gasser, G.; Furrer, J. Characterization of the activities of dinuclear thiolato-bridged arene ruthenium complexes against *Toxoplasma gondii*. *Antimicrob. Agents Chemother.* **2017**, *61*, e01017–e01031. [\[CrossRef\]](#)

91. Jelk, J.; Balmer, V.; Stibal, D.; Giannini, F.; Süss-Fink, G.; Butikofer, P.; Furrer, J.; Hemphill, A. Anti-parasitic dinuclear thiolato-bridged arene ruthenium complexes alter the mitochondrial ultrastructure and membrane potential in *Trypanosoma brucei* bloodstream forms. *Exp. Parasitol.* **2019**, *205*, 107753. [\[CrossRef\]](#)
92. Giannini, F.; Bartoloni, M.; Paul, L.E.H.; Süss-Fink, G.; Reymond, J.-L.; Furrer, J. Cytotoxic peptide conjugates of dinuclear areneruthenium trithiolato complexes. *Med. Chem. Commun.* **2015**, *6*, 347–350. [\[CrossRef\]](#)
93. Desiatkina, O.; Paunescu, E.; Mosching, M.; Anghel, N.; Boubaker, G.; Amdouni, Y.; Hemphill, A.; Furrer, J. Coumarin-tagged dinuclear trithiolato-bridged ruthenium(II)-arene complexes: Photophysical properties and antiparasitic activity. *ChemBioChem* **2020**, *21*, 2818–2835. [\[CrossRef\]](#) [\[PubMed\]](#)
94. Desiatkina, O.; Boubaker, G.; Anghel, N.; Amdouni, Y.; Hemphill, A.; Furrer, J.; Paunescu, E. Synthesis, photophysical properties and biological evaluation of new conjugates BODIPY—Dinuclear trithiolato-bridged ruthenium(II)-arene complexes. *ChemBioChem*, 2022; in press. [\[CrossRef\]](#) [\[PubMed\]](#)
95. Stibal, D.; Therrien, B.; Süss-Fink, G.; Nowak-Sliwinska, P.; Dyson, P.J.; Cermakova, E.; Rezacova, M.; Tomsik, P. Chlorambucil conjugates of dinuclear p-cymene ruthenium trithiolato complexes: Synthesis, characterization and cytotoxicity study in vitro and in vivo. *J. Biol. Inorg. Chem.* **2016**, *21*, 443–452. [\[CrossRef\]](#)
96. Desiatkina, O.; Johns, S.K.; Anghel, N.; Boubaker, G.; Hemphill, A.; Furrer, J.; Păunescu, E. Synthesis and antiparasitic activity of new conjugates-organic drugs tethered to trithiolato-bridged dinuclear ruthenium(II)-arene complexes. *Inorganics* **2021**, *9*, 59. [\[CrossRef\]](#)
97. Liang, L.; Astruc, D. The copper(I)-catalyzed alkyne-azide cycloaddition (CuAAC) “click” reaction and its applications. An overview. *Coord. Chem. Rev.* **2011**, *255*, 2933–2945. [\[CrossRef\]](#)
98. Meldal, M.; Tornøe, C.W. Cu-catalyzed azide-alkyne cycloaddition. *Chem. Rev.* **2008**, *108*, 2952–3015. [\[CrossRef\]](#)
99. Zhang, W.Y.; Banerjee, S.; Imberti, C.; Clarkson, G.J.; Wang, Q.; Zhong, Q.; Young, L.S.; Romero-Canelon, I.; Zeng, M.; Habtemariam, A.; et al. Strategies for conjugating iridium(III) anticancer complexes to targeting peptides via copper-free click chemistry. *Inorg. Chim. Acta* **2020**, *503*, 119396. [\[CrossRef\]](#) [\[PubMed\]](#)
100. Farrer, N.J.; Griffith, D.M. Exploiting azide-alkyne click chemistry in the synthesis, tracking and targeting of platinum anticancer complexes. *Curr. Opin. Chem. Biol.* **2020**, *55*, 59–68. [\[CrossRef\]](#)
101. Zabarska, N.; Stumper, A.; Rau, S. CuAAC click reactions for the design of multifunctional luminescent ruthenium complexes. *Dalton Trans.* **2016**, *45*, 2338–2351. [\[CrossRef\]](#)
102. Wang, X.; Zhu, M.; Gao, F.; Wei, W.; Qian, Y.; Liu, H.K.; Zhao, J. Imaging of a clickable anticancer iridium catalyst. *J. Inorg. Biochem.* **2018**, *180*, 179–185. [\[CrossRef\]](#)
103. Ganesh, V.; Sudhir, V.S.; Kundu, T.; Chandrasekaran, S. 10 years of click chemistry: Synthesis and applications of ferrocene-derived triazoles. *Chem. Asian J.* **2011**, *6*, 2670–2694. [\[CrossRef\]](#)
104. Singh, G.; Arora, A.; Kalra, P.; Maurya, I.K.; Ruiz, C.E.; Estebanc, M.A.; Sinha, S.; Goyal, K.; Sehgal, R. A strategic approach to the synthesis of ferrocene appended chalcone linked triazole allied organosilatrane: Antibacterial, antifungal, antiparasitic and antioxidant studies. *Bioorg. Med. Chem.* **2019**, *27*, 188–195. [\[CrossRef\]](#) [\[PubMed\]](#)
105. Kumar, K.; Carrere-Kremer, S.; Kremer, L.; Guerardel, Y.; Biot, C.; Kumar, V. Azide-alkyne cycloaddition en route towards 1H-1,2,3-triazole-tethered beta-lactam-ferrocene and beta-lactam-ferrocenylchalcone conjugates: Synthesis and in vitro anti-tubercular evaluation. *Dalton Trans.* **2013**, *42*, 1492–1500. [\[CrossRef\]](#) [\[PubMed\]](#)
106. Singh, A.; Viljoen, A.; Kremer, L.; Kumar, V. Azide-alkyne cycloaddition en route to 4-aminoquinoline-ferrocenylchalcone conjugates: Synthesis and anti-TB evaluation. *Future Med. Chem.* **2017**, *9*, 1701–1708. [\[CrossRef\]](#)
107. Kroll, A.; Monczak, K.; Sorsche, D.; Rau, S. A luminescent ruthenium azide complex as a substrate for copper-catalyzed click reactions. *Eur. J. Inorg. Chem.* **2014**, *2014*, 3462–3466. [\[CrossRef\]](#)
108. Karmis, R.E.; Carrara, S.; Baxter, A.A.; Hogan, C.F.; Hulett, M.D.; Barnard, P.J. Luminescent iridium(III) complexes of N-heterocyclic carbene ligands prepared using the ‘click reaction’. *Dalton Trans.* **2019**, *48*, 9998–10010. [\[CrossRef\]](#)
109. Mandal, S.; Das, R.; Gupta, P.; Mukhopadhyay, B. Synthesis of a sugar-functionalized iridium complex and its application as a fluorescent lectin sensor. *Tetrahedron Lett.* **2012**, *53*, 3915–3918. [\[CrossRef\]](#)
110. Kolb, H.C.; Sharpless, K.B. The growing impact of click chemistry on drug discovery. *Drug Discov. Today* **2003**, *8*, 1128–1137. [\[CrossRef\]](#) [\[PubMed\]](#)
111. Păunescu, E.; Boubaker, G.; Desiatkina, O.; Anghel, N.; Amdouni, Y.; Hemphill, A.; Furrer, J. The quest of the best—A SAR study of trithiolato-bridged dinuclear ruthenium(II)-arene compounds presenting antiparasitic properties. *Eur. J. Med. Chem.* **2021**, *222*, 113610. [\[CrossRef\]](#)
112. Păunescu, E.; Louise, L.; Jean, L.; Romieu, A.; Renard, P.-Y. A versatile access to new halogenated 7-azidocoumarins for photoaffinity labeling: Synthesis and photophysical properties. *Dyes Pigm.* **2011**, *91*, 427–434. [\[CrossRef\]](#)
113. Kitamura, M.; Kato, S.; Yano, M.; Tashiro, N.; Shiratake, Y.; Sando, M.; Okauchi, T. A reagent for safe and efficient diazo-transfer to primary amines: 2-azido-1,3-dimethylimidazolium hexafluorophosphate. *Org. Biomol. Chem.* **2014**, *12*, 4397–4406. [\[CrossRef\]](#)
114. Beckmann, H.S.; Wittmann, V. One-pot procedure for diazo transfer and azide-alkyne cycloaddition: Triazole linkages from amines. *Org. Lett.* **2007**, *9*, 1–4. [\[CrossRef\]](#) [\[PubMed\]](#)
115. Roy, B.; Dutta, S.; Choudhary, A.; Basak, A.; Dasgupta, S. Design, synthesis and RNase A inhibition activity of catechin and epicatechin and nucleobase chimeric molecules. *Bioorg. Med. Chem. Lett.* **2008**, *18*, 5411–5414. [\[CrossRef\]](#) [\[PubMed\]](#)

116. Vo, D.D.; Duca, M. *Design of Multimodal Small Molecules Targeting miRNAs Biogenesis: Synthesis and In Vitro Evaluation*; Schmidt, M.F., Ed.; Springer: New York, NY, USA, 2017.
117. Krim, J.; Taourirte, M.; Engels, J.W. Synthesis of 1,4-disubstituted mono and bis-triazolocarbo-acyclonucleoside analogues of 9-(4-hydroxybutyl)guanine by Cu(I)-catalyzed click azide-alkyne cycloaddition. *Molecules* **2011**, *17*, 179–190. [[CrossRef](#)] [[PubMed](#)]
118. Lolk, L.; Pohlsgaard, J.; Jepsen, A.S.; Hansen, L.H.; Nielsen, H.; Steffansen, S.I.; Sparving, L.; Nielsen, A.B.; Vester, B.; Nielsen, P. A click chemistry approach to pleuromutilin conjugates with nucleosides or acyclic nucleoside derivatives and their binding to the bacterial ribosome. *J. Med. Chem.* **2008**, *51*, 4957–4967. [[CrossRef](#)]
119. Krim, J.; Sillahi, B.; Taourirte, M.; Rakib, E.M.; Engels, J.W. Microwave-assisted click chemistry: Synthesis of mono and bis-1,2,3-triazole acyclonucleoside analogues of Acyclovir via copper(I)-catalyzed cycloaddition. *ARKIVOC* **2009**, *2009*, 142–152. [[CrossRef](#)]
120. Lindsell, W.E.; Murray, C.; Preston, P.N.; Woodman, T.A.J. Synthesis of 1,3-diynes in the purine, pyrimidine, 1,3,5-triazine and acridine series. *Tetrahedron* **2000**, *56*, 1233–1245. [[CrossRef](#)]
121. Rocha, D.H.A.; Machado, C.M.; Sousa, V.; Sousa, C.F.V.; Silva, V.L.M.; Silva, A.M.S.; Borges, J.; Mano, J.F. Customizable and regioselective one-pot N–H Functionalization of DNA nucleobases to create a library of nucleobase derivatives for biomedical applications. *Eur. J. Org. Chem.* **2021**, *2021*, 4423–4433. [[CrossRef](#)]
122. Zhang, X.; Liu, P.; Zhu, L. Structural determinants of alkyne reactivity in copper-catalyzed azide-alkyne cycloadditions. *Molecules* **2016**, *21*, 1697. [[CrossRef](#)]
123. Kokina, A.; Ozolina, Z.; Liepins, J. Purine auxotrophy: Possible applications beyond genetic marker. *Yeast* **2019**, *36*, 649–656. [[CrossRef](#)]
124. Giannini, F.; Furrer, J.; Ibao, A.F.; Süss-Fink, G.; Therrien, B.; Zava, O.; Baquie, M.; Dyson, P.J.; Stepnicka, P. Highly cytotoxic trithiophenolatodiruthenium complexes of the type [(eta6-p-MeC6H4Pri)2Ru2(SC6H4-p-X)3]+: Synthesis, molecular structure, electrochemistry, cytotoxicity, and glutathione oxidation potential. *J. Biol. Inorg. Chem.* **2012**, *17*, 951–960. [[CrossRef](#)] [[PubMed](#)]
125. Giannini, F.; Süss-Fink, G.; Furrer, J. Efficient oxidation of cysteine and glutathione catalyzed by a dinuclear areneruthenium trithiolato anticancer complex. *Inorg. Chem.* **2011**, *50*, 10552–10554. [[CrossRef](#)]
126. Anghel, N.; Muller, J.; Serricchio, M.; Jelk, J.; Butikofer, P.; Boubaker, G.; Imhof, D.; Ramseier, J.; Desiatkina, O.; Paunescu, E.; et al. Cellular and molecular targets of nucleotide-tagged trithiolato-bridged arene ruthenium complexes in the protozoan parasites *Toxoplasma gondii* and *Trypanosoma brucei*. *Int. J. Mol. Sci.* **2021**, *22*, 10787. [[CrossRef](#)] [[PubMed](#)]
127. McFadden, D.C.; Seeber, F.; Boothroyd, J.C. Use of *Toxoplasma gondii* expressing beta-galactosidase for colorimetric assessment of drug activity in vitro. *Antimicrob. Agents Chemother.* **1997**, *41*, 1849–1853. [[CrossRef](#)]
128. Studer, V.; Anghel, N.; Desiatkina, O.; Felder, T.; Boubaker, G.; Amdouni, Y.; Ramseier, J.; Hungerbühler, M.; Kempf, C.; Heverhagen, J.T.; et al. Conjugates containing two and three trithiolato-bridged dinuclear ruthenium(II)-arene units as in vitro antiparasitic and anticancer agents. *Pharmaceuticals* **2020**, *13*, 471. [[CrossRef](#)] [[PubMed](#)]
129. Muller, J.; Aguado-Martinez, A.; Manser, V.; Balmer, V.; Winzer, P.; Ritler, D.; Hostettler, I.; Arranz-Solis, D.; Ortega-Mora, L.; Hemphill, A. Buparvaquone is active against *Neospora caninum* in vitro and in experimentally infected mice. *Int. J. Parasitol. Drugs Drug. Resist.* **2015**, *5*, 16–25. [[CrossRef](#)]
130. Vo, D.D.; Duca, M. *Drug Target miRNA: Methods and Protocols*; Schmidt, E.M.F., Ed.; Springer: New York, NY, USA, 2017; pp. 137–154.
131. Giannini, F.; Furrer, J.; Süss-Fink, G.; Clavel, C.M.; Dyson, P.J. Synthesis, characterization and in vitro anticancer activity of highly cytotoxic trithiolato diruthenium complexes of the type [(eta6-p-MeC6H4iPr)2Ru2(mu2-SR1)2(mu2-SR2)]+ containing different thiolato bridges. *J. Organomet. Chem.* **2013**, *744*, 41–48. [[CrossRef](#)]
132. Jansa, P.; Špaček, P.; Votruba, I.; Břehová, P.; Dračinský, M.; Klepetářová, B.; Janeba, Z. Efficient one-pot synthesis of polysubstituted 6-[(1H-1,2,3-triazol-1-yl)methyl]uracils through the “click” protocol. *Collect. Czech. Chem. Commun.* **2011**, *76*, 1121–1131. [[CrossRef](#)]
133. Fulmer, G.R.; Miller, A.J.M.; Sherden, N.H.; Gottlieb, H.E.; Nudelman, A.; Stoltz, B.M.; Bercaw, J.E.; Goldberg, K.I. NMR chemical shifts of trace impurities: Common laboratory solvents, organics, and gases in deuterated solvents relevant to the organometallic chemist. *Organometallics* **2010**, *29*, 2176–2179. [[CrossRef](#)]